DOI: https://doi.org/10.38027/ICCAUA2023EN0003

LULC geospatial OLI/Landsat -7 -8 -9 analysis of Sitakunda Container Depot: MLE and Kappa accuracy for Coastal Urban Sprawl and Infrastructure Change.

Ing. Arch. **Salvatore Polverino** [1], Arch. **Antonio Coppola** [2]
Dipartimento Formazione ed Internazionalizzazione, Ordine Architetti Pianificatori Paesaggisti Conservatori di Napoli e Provincia, Napoli, Italy
E-mail : formazione@napoli.archiworld.it [1,2], polverinosalvatore@outlook.com [1]

Abstract
The extent of this research aims to demonstrate a Land Use/Land Cover (LULC) change over a coastal-industrial area of Sitakunda, part of Chittagong region in Bangladesh. Its reference information has included important drivers for this industrial area of 4.00 km^2, that highlight its suburban growth that uncontrollably has disaggregated the rural landscape, in a period ranging from 2009 to 2022. Our geospatial analysis has started with the observation of the BM Container Warehouse, that has been recently interested by a dreadful fire.
Supervised Maximum Likelihood classifier has been yearly applied, with regard of six landscape drivers that were interpretated as: Built Up (BU) Terminal, BU Infrastructure, BU Other Deports, BU Ancillary/Generic, Vegetation/Barren Land and Forest. The Landsat/OLI (Operational Land Imager -7 -8 -9 programs) based sampling of 117 ground points on the basis of Google Earth's Imagery, has provided different level 1 land cover records, with the advantage of a 15 meters panchromatic definition. Kappa (K) coefficients have also coordinated our geospatial investigation: (1) for BM commercial expansion, a 0.84 % larger than the initial perimeter of construction (2009-July 2022), a 8.79 % (2014-July 2022), a 2.12 % (2017-July 2022); (2) for the general BU Infrastructure, important ramifications, broader than they seemed at first glance, increased by a 3.39 % (2009-July 2022); (3) for BU Other Depots rise, 9.64 % (2014-July 2022); (4) for BU Ancillary escalation, an amplified increase by 19.53 % (2009-July 2022); subsequently we assessed the diminishing of Vegetation/Barren land, -2.61 % (2009-July 2022) together with the Forest, 0.15 %, during the same period. Preceding this object-based classification, other accuracy statistics, highlighted by Pearson correlation, have showed us partial inconsistencies (class a <0.30 r^2)affecting certain coastal features, e.g. Ancillary two-year 2013-2014 [275.18, -217.22 %], yearly interested by monsoon seasons, so that our ground-truth references did not fully meet the percentual integrity within K and Overall Accuracy (OA) $q_{1/4}$- $q_{1/3}$ thresholds [47.59, 94.54 %], and [47.59, 95.68 %]. Pattern irregularity of the Indian-bengali Landscape Architecture (LA) has been conclusively interpretated with regard of the infrastructure variation, as an integral part of Life Cycle Assessment (LCA), using the minimum Euclidean distance, by iterating such Unsupervised Classification clustering procedure, between the most convenient pre-date 2022 fire OLI dataset (May), and the earliest post-date fire (July). The research, apart from the validation study, has also listed the inter-class spectral separability analysis, herewith yearly distributed, based on the Maximum Likelihood Classification (MLE) Composite bands classification and its firms, in correlation with related linear regression, resulting from the early LA stage of approach.
Keywords: International Safety Management Code; Digital forensics; LULC; Remote sensing; Fire Risk; Life Cycle Assessment (LCA); Environmental Impact Assessment (EIA); Strategic Environmental Assessment (SEA): Port area; Logistics; Coastal settlements; Habitat II United Nations.

1. Introduction

1.1. Causes of ignition: fire, explosions and casualties

The region of interest of our case study, is limited to a peri-urban rectangular boundary, in Sitakunda, Chittagong region of Bangladesh; the extension amounts to nearly 4.00 square km, with the exclusion of the adjacent seawaters. BM sub-area covers an area of round about 92,644 m^2, with a perimeter of 1,242 meters, localized at 91°70'00 Long 22°47'00 Lat, according to the local UTM for Bangladesh. The purpose of our department research is partially aimed to follow an emerging Wildland-Urban Interface (WUI) model (McNamara et Mell, 2022) in order to produce, surveyal and/or remote-sensed/airborne consistency, backed up by statistical reporting, aimed to the technical identification of those surface variations with regard of building destruction, fire behavior and LA defensive actions (Mohamed A. et al., 2022). The combustion was estimated to have started with the unpredictable reaction of igneous garments and chemicals at 21:00 BST (15:00 UTC) following a first explosion at 23:45 BST (17:45 UTC), in the matter of fireballs debris. The object of ignition was detected by the Bangladesh Fire Service & Civil Defense, as to be highly flammable garments and chemicals (Wadud Z. et al., 2014). In last instance the forensics (Kuveždić D. et al., 2020), operated by Bangladesh's fire service, concluded by confirming that the unpredictable spread was initiated by hydrogen peroxide presence, stored in several slots around the terminal. The bidimensional design of this highly density Terminal, did not consent an urgent search & rescue (SAR) (Barua U. et al., 2018), due to the narrowness of its unique entrance, with the paralysis of complex operational units' vehicles, suffocated by the stagnation of deadly smoke curtains. Firefighters' anxiety, herewith trapped in a such urban congestion (Saini V., 2020), caused improper decisional choices by extinguishing normal water in a D-class scenario (European Committee for Standardization – CEN), characterized by metallic substances (i.e., sodium, potassium, aluminum), rather than special dusty fireproof matters.

Figure 1. Pre-date fire entrance: unique gateway of access.

Figure 2. Pre-date fire goods: heterogeneity of sorting.

Figure 3. Pre-date fire Ro-Ro gateway: unique provincial road.

Figure 4. Post-date fire Terminal rogue: decisional unawareness.

Figure 5. Post-date fire Firefighters: improper usage of Water.

Figure 6. Post-date fire Terminal: water bowls scattered on site.

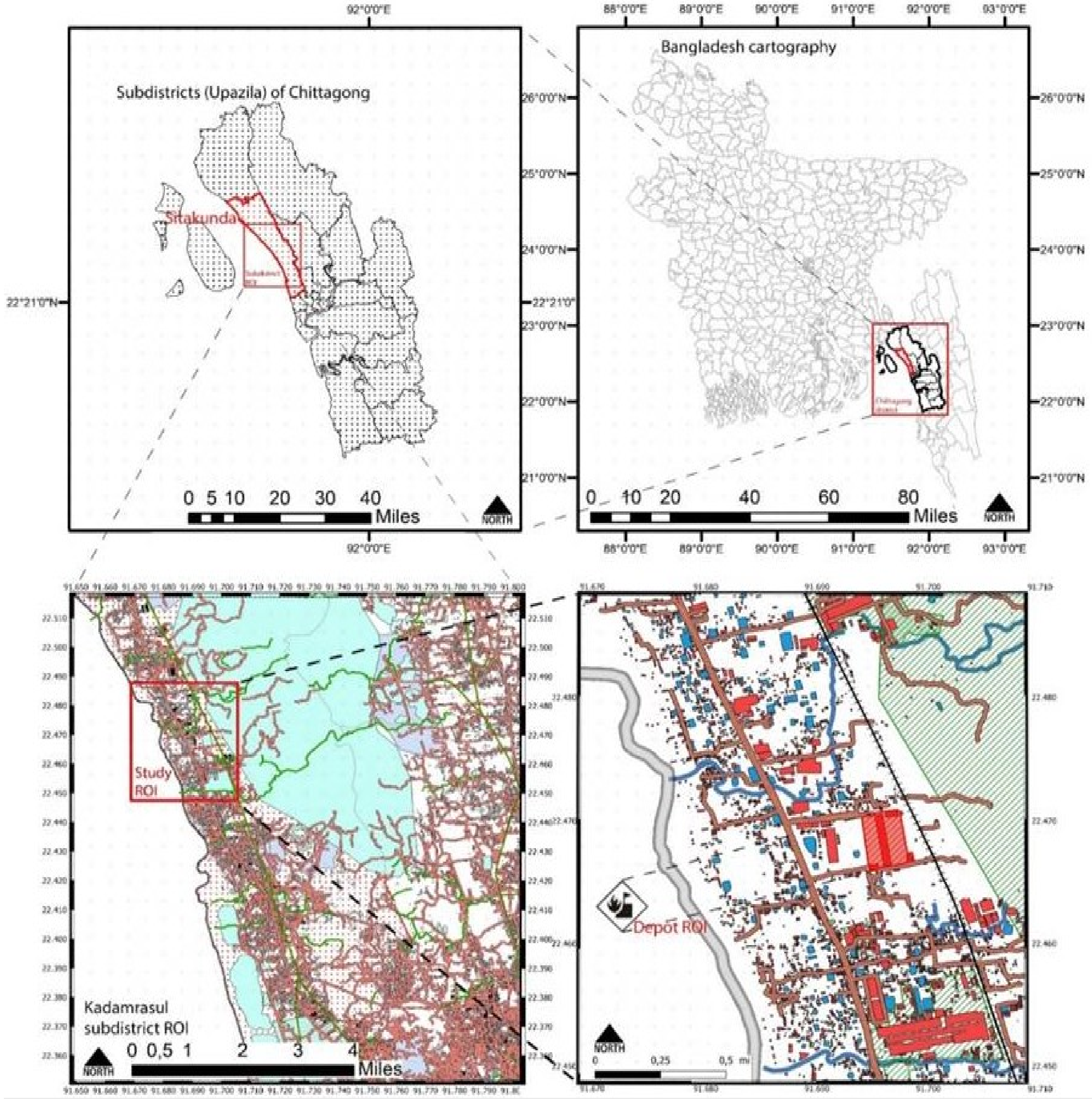

Figure 7. Mosaic of Geographic Information System (GIS) chartography to illustrate this survey case investigation.

BU Terminal
The rectangular shaped covered roof warehouse that constitutes the core of this BM Container Depot Limited Terminal. This land-cover has a specific accountability with regard of this case study.

BU Infrastructure
All metal and asphalt covered areas that determine the entropy of such anthropic activities. The heterogeneity of this type includes piles of industrial spare parts as well as fishing and farming machineries, apart from Kashem Jute Mills Ltd.

BU Other Depots
All covered areas belonging to industrial stakeholders, secondarily accounted for this case study: Abul Khair Steel Industries, AKSML Power Substation, Arif, Shema Oxygen Oxico Ltd, Infinia Composite Textiles Ltd and Infinia Spinning Mills.

BU Ancillary/Generic Purpose
All covered spaces attributed to fragmented residential/processing/tertiaty sector based edifices, with the inclusion of adjacent yards and heterogeneous pieces of machineries.

Vegetation/Barren land
All Grass, sand covered areas with the supervised classification of natural grassland (i.e. shrubs and swamps) together with productive soil.

Forest
All forestry covered areas with the supervised classification of both spontaneous planted woodland and wild timber land.

Table 1. LULC Categorization.

Figure 8. BU Core Terminal.

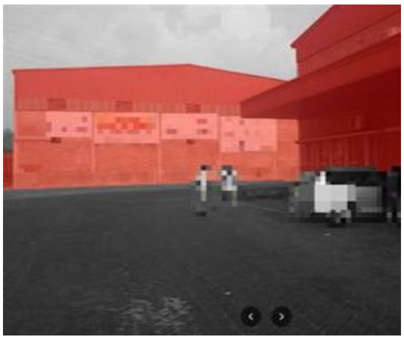

Figure 9. BU Depot Terminal.

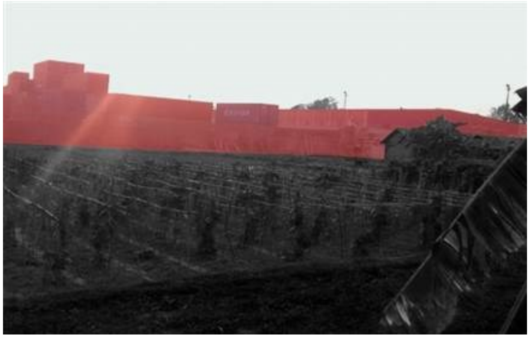

Figure 10. BU Terminal and adjacent railway.

Figure 11. AKSPL Steel Industry.

Figure 12. Barren coastal land.

Figure 13. Coastal settlement object.

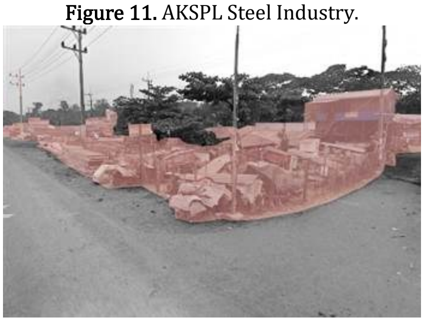

Figure 14. Main avenue and its infrastructural sprawl.

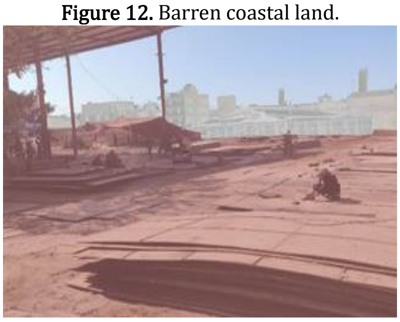

Figure 15. Infrastructural sprawl and its entropy.

Figure 16. Vegetation mixed use, also subtracted by the Forest canopy.

1.2. Final Report, 2018, and Dangerous Cargoes Act V, 1953.

In the history of the country, we accounted two main documents that set the basis of a respectful and modern urban discipline in Bangladesh, with regard of logistical, operational and storage of dangerous cargoes, In first instance the Dangerous Cargoes, signed in 1953, followed by a Data Collection Survey (Nippon K. et al., 2018) set an extensive groundwork, structurally engineered in favour of a modern Bangladesh: Energy sector has been mainly addressed to domestic natural gas, in the matter of the national “back-born” of priority significance, followed by a general declining demand of production so that the actual stakeholders will learn how to differentiate the production chains in the immediate future according to EU legislations (Islam D. et al., 2022, Rahman K, 2021, Razzaque M. et al., 2019, Amen, 2021).

In this paragraph, we decided to underline the executive briefing by two Japanese authorships, signed by Nippon Koei Co., Ltd. and Chiyoda U-tech Co., Ltd, due to a power station presence allocated within the projected ROI, in parallel with the ultimation of its adjacent steel industrial heavy complex. The research (2009-2022) visualizes auxiliary pipelines in progress, that are part of the Network Infrastructure Management System, sub-part of Power Sector Master Plan 2016. The distribution systems for liquified natural gas (LNG) introduction, is clearly demonstrated with the Chapter 5, and ruled by the Ministry of Power, Energy and Mineral Resources (MoPEMR), subdivided into: 1) Energy and Mineral Resources Division (EMRD), and 2) Power Division (PD). The latter was reviewed in six bodies: I) Power Cell; II) Bangladesh Power Development Board (BPDB); III) Bangladesh Rural

Electrification Board (BREB); IV) Power Grid Company of Bangladesh (PGCB); V) Distribution companies; VI) Power generation companies.
The substation herewith sensed, relies on the Karnaphuli Gas Distribution Company Limited (KGDCL), whose effort currently is aimed to the development of a Maintenance culture in Bangladesh (Department of Sociology, 2018), together with the fire prevention; both disciplines lack of awareness with alarming concern (The Hazardous Wastes and Shipbreaking Waste Management Rules, 2011), and determined two factors in our research: the first is remarkable issued by the uncontrolled urban sprawl of the naval-coastal settlement (Alam S. et al., 2014, Rahman K. et al., 2019, Thron C. et al., 2015), also generating "impromptu" in the matter of ship breaking yards (Abdullah et al., 2013, Tuhin T. et al., 2020, Amen & Nia, 2020) and the eradication of ancillary cover type in occasion of monsoon seasons (Uddin K. et al., 2003); whilst the second tendency was benchmarked with higher index accuracy percentage values, over an exponential upgrade of other industrial facilities, sampled on the basis of bluish roof colour, infrastructures (Bangladesh University, 2012), i.e. roads, metallic surfaces also including the adjacent warehouse to the BM Terminal, and ancillary general built up (residential) cover type. Vegetation and Forest classes have seen an overall diminishing, so that we also included climate resilient and participatory reforestation projects (Bangladesh Forest Department, 2016). With specific regard of the Power Station, the study limited the geospatial analysis to the level 1 LULC, because of the high handwork to assess such an extensive area, in a temporal range, covering over a decade of transformations; the effort herewith demonstrated, was partially also dedicated to the displacing of technical types of accuracy information. Indeed, following in-depth levels might benchmark smaller scales of sensing. According to these limits of research, the 15 meters definition level 1, consented us to confine the careful excavation site around the substation; to mention Final Report (2018): "These pipeline systems need to be monitored and investigated carefully and need to be replaced with appropriate materials to avoid potential rupture case"– "These pipeline systems need to be monitored and investigated carefully and need to be replaced with appropriate materials to avoid potential rupture case" – Design Classification: "Design classification is related to thickness of pipe, specified according to population. Current population and future development plan need to be considered prior to decide classification and determined during Environmental Impact Assessment (EIA)" – Soil Resistivity: "CP system may differ to the soil resistivity and condition. Data should be prepared and verified as part of EIA".
An infrastructural improvement has impacted positively around the peri-urban industrial complex, by expanding the need of standardization (People's Republic of Bangladesh Ministry of Power, Energy and Mineral, 2018) in favour of the: 1a) Civil sector (Road, Railway, Cable/Pipeline, Water Course, River, River Crossing); 1b) Site Construction sector (Road, Pavement, Boundary Wall and Gate, Fence, Trench, Drainage, Concrete Foundations, Valve Pit, Valve Pit Cover, Pig Trap Foundation); 2) Piping (Pipe Support Standard, Welding Details, Scraper Trap, Pig Launcher and Receiver, Scraper Signaler, Vent and Drain Piping at Valve Station); 3) Instrumental sector; 4) Electrical sector; 5) Grounding Ion System sector. At page 48 of the report, an intermodal Gas Operation Mode to Demand Base is also conceptualized, with three out-puts from the LNG framework: 1) Power Plant and City Gas/Transport/Industry; 2) Cities; 3) Cities/Power Plant. The concern is aimed to the prevention of bottlenecks, losses, general corrosion/ground stability. Another Level 1/Documental limit, consist of the impossibility to determining whether certain industries are connected via virtual database or not. In the future this linkage would be presumably extended also to residential and minor stakeholders, as the Power Sub-Division Organization aims to, by promoting "public-private partnership, private investment rural electrification and renewable energy, and energy efficiency and conservation". The most tangible example of this bottom-up (Islam N. et al., 2022) positive impact, is the Bangladesh Rural Electrification Board (BREB, here BPDB South Zone) est. in 1977, in 2016 including over 14 million customers in the country.
The oldest report herewith considered, is the Dangerous Cargoes Act V, est. in 1953 (provided by: FAO/FAOLEX/ECOLEX Database, Food and Agriculture Organization of the United Nations) whose jurisdiction was extended exclusively to the pertinent territory of Bangladesh. The novel importance, at that time, was referred to the fact that: 1) "any goods shown as Explosives in the Comprehensive Classified List of Government Explosives compiled and issued by the Government or by such authority as the Government may determine from time to time or any ammunitions; or (b) petroleum, as defined in clause (a) of section 2 of the Petroleum Act, 1934, when the flashing point of such petroleum is below one hundred and fifty degrees Fahrenheit" – 2) "Fortress Commander" means an officer of the armed forces appointed as such by the Government by a notification in the official Gazette -3) "The Government may make such orders as appear to it to be necessary or expedient for securing the safety of any port and preventing or dealing with explosions and fires on vessels carrying dangerous cargoes within the limits of any port, and generally for the transit working and storage of dangerous cargoes and matters incidental".

2. Methodology

2.1. Workflow

The basic strategy of this urban pattern recognition is to assess LULC visually and quantitatively with the implementation of the Esri© package (Hussain S. et al., 2022, Saha P. et al., 2022, Aziz Amen, 2022, Amen et al., 2023), grouping sample data and putting them into practice with traditional algorithm land cover classified maps (Acharya T. et al., 2018). Each year is selected according to the criteria that do not affect from the cloud also considering the monsoon season, we hence moved into preferring the winter period. To maintain validity of the targeted sites, we used the blue, green, red, near-infrared (NIR) bands for image classification. The following stacks present three columns: 1) a color composites raster (R: Red band, B: Blue band, G: Green band), 2) a 5-1-3 combination, 3) the resulting LULC model. At this current stage, the department is focused on kappa accuracy methodology, we hence assumed to propose a visual graphic and quantitative set of information, that cover this area of research in the built and rural environment. Locations have been all set within the same frame in ArcGIS software as well as the accuracy points that amount between 115 and 117 per year, and mainly allocated in correspondence to the BM Terminal. The criteria necessary to produce their producer accuracy validation (Humayun K., 2012) a have seen the consulting of Google Earth Pro historical imagery, with 1610 validation samples, 14 User Accuracy Confusion matrixes, 14 Producer Accuracy Confusion matrixes, always accounting both six reference and classified data. In the very end of this dissertation, we concluded to confront, via Unsupervised classification, the infrastructure areal change, (Wang R. et al., 2021) by setting the pre- and post-date fire LULC maps (Polverino S., 2022) both presenting a solid Kappa and Overall percentage also supported by correctly classified and reference pixels, as the auxiliary inputs due to their relative consistency to the premise model before aforementioned. The visual consistency generated a large set of clusters, (Matlhodi B. et al., 2019) that match with the differenced LULC and let us comprehend which actions by local inhabitants were taken, in the exact period occurring after the fire of BM Terminal.

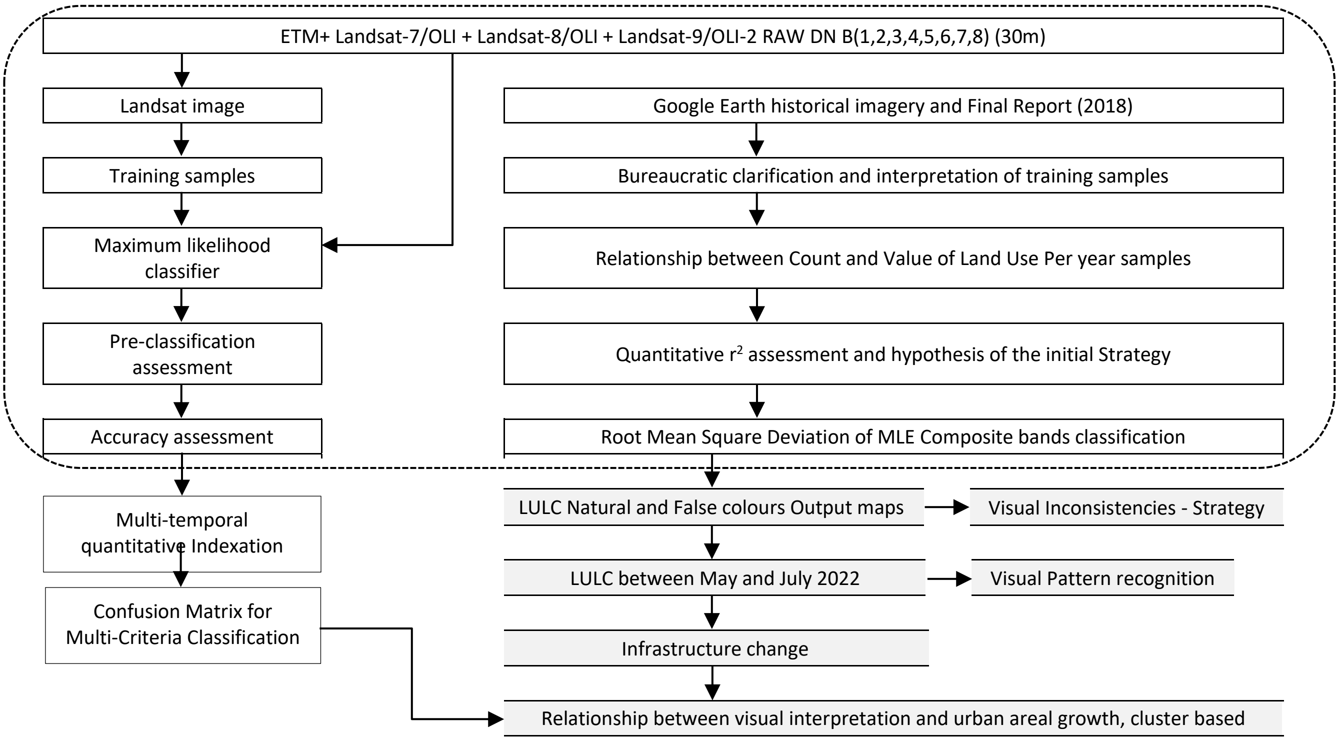

Figure 17. Flow diagram of the image processing and its statistical analysis techniques. The proposed geospatial approach has taken into account both Supervised and Unsupervised Classification methods. Apart the spectral and quantitative analysis, we accounted a selection of qualitative approaches that are addressed to the discipline of Landscape Architecture for our department.

Table 2. Landsat data used in this study (https://landsat.gsfc.nasa.gov/appendix/references).

	Bands		Spatial Resolution (m)	Wavelength (μm)
Landsat 7 Enhanced Thematic Mapper Plus (ETM+)	1	Blue	30	0.45–0.52
	2	Green	30	0.52-0.60
	3	Red	30	0.63-0.69
	4	Near Infrared (NIR)	30	0.77-0.90
	5	Shortwave Infrared SWIR 1	30	1.55-1.75
	6	Thermal	60* (30)	10.40-12.50
	7	Shortwave Infrared (SWIR) 2	60	2.09-2.35
	8	Panchromatic	15	.52-.90
Landsat 8/9 OLI	1	Ultra-Blue (coastal/aerosol)	30	0.435 - 0.451
	2	Blue	30	0.452 - 0.512
	3	Green	30	0.533 - 0.590
	4	Red	30	0.636 - 0.673
	5	Near Infrared (NIR)	30	0.851 - 0.879
	6	Shortwave Infrared (SWIR)	30	1.566 - 1.651
	7	Shortwave Infrared (SWIR) 2	30	2.107 - 2.294
	8	Panchromatic	15	0.503 - 0.676

Table 3. Summary of Landsat datasets performed to carry out the analysis.

ID	Image Name	Path	Row	Year	Month	Day	Cloud coverage
1	LE07_L1TP_136045_20091214_20200911_02_T1	136	045	2009	12	14	3.00
2	LE07_L1TP_136045_20101217_20200910_02_T1	136	045	2010	12	17	0.00
3	LE07_L1TP_136044_20111204_20200909_02_T1	136	044	2011	12	04	32.00
4	LE07_L1TP_136044_20121206_20200908_02_T1	136	044	2012	12	06	3.00
5	LC08_L2SP_136045_20131030_20200912_02_T1	136	045	2013	10	30	1.23
6	LC08_L2SP_136044_20141220_20200910_02_T1	136	044	2014	12	20	1.65
7	LC08_L2SP_136045_20151223_20200908_02_T1	136	045	2015	12	23	0.02
8	LC08_L2SP_136045_20161225_20200905_02_T1	136	045	2016	12	25	1.48
9	LC08_L1TP_136044_20171126_20200902_02_T1	136	045	2017	12	28	5.66
10	LC08_L2SP_136045_20181231_20200830_02_T1	136	045	2018	12	31	0.01
11	LC08_L2SP_136045_20191218_20201023_02_T1	136	045	2019	12	18	0.68
12	LC08_L2SP_13604 4_20201204_2021 0313_02_T1	136	044	2020	12	04	1.97
13	LC09_L2SP_136045_20211215_20220120_02_T1	136	045	2021	12	15	9.20
		Pre-date Fire Assessment					
14	LC08_L2SP_136045_20220516_20220519_02_T1	136	045	2022	05	16	79.80
		Post-date Fire Assessment					
15	LC09_L2SP_136045_20220727_20220729_02_T1	136	045	2022	07	27	9.65

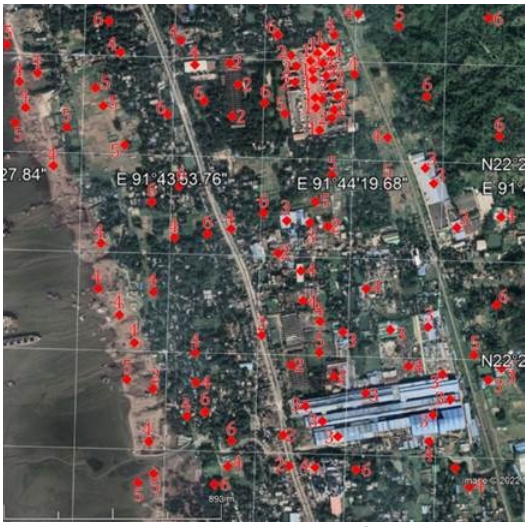

Figure 18. LULC User points, July 2022.

Table 4. Summary of input samples.

Class	Visual consistency	N°	Year
BU Terminal [1]	Red metallic roof	9	2011
BU Infrastructure [2]	Metallic surfaces (including open structures with raw goods, i.e. landfills).	22	2009
BU Other Depots [3]	Blue metallic surfaces of the steel industry, its satellite structures.	18	2009
BU Ancillary/Generic [4]	Grey structures consisting in residential et similia.	33	2009
BU Vegetation/Barren [5]	Bright green or soil without shadows, agricultural/wild.	16	2009
BU Forest [6]	Battered green with shadows, also riverside.	17	2009

2.2. Non-linear correlation in addition to a preliminary insight.

The visualization of linear regression from the resulting LULC outputs, has been considered in a 2017 paper (Tran, D. X. et al., 2017); herewith, the authors underline its general tendency to the future prediction of the following morphology heterogeneity together with the land cover data variability (Feizizadeh B. et al., 2022, Cai G. et al., 2019, Foody G. et al., 2010, 2020). Therefore, we grouped four value thresholds in relation to LULC changes, to allocate the suitable LA strategies (Rosenfield G. H. et al., 1986) to be interpretated (Congalton R. et al., 1983, 2001), as the impact mitigator guidelines of the urban acknowledges, yearly listed as follows.

Table 5.1 Relationship between Count and Value of Land Use Land Cover per year samples.

Data	Classification method	Cover types	Equation	Linear regression [r^2]	Strategy
LE07_L1TP_136045_20091214_20200911_02_T1	Pixel-based method	Built Up Terminal Built Up Infrastructure Built Up Other Depots Built Up Ancillary/Gen. Vegetation/Barren land Forest	$y = 10.9 + 0.0066\ x$	0.15	(Casamonti M., 2006) (Pontius G. et al., 2011) (Nippon K. et al., 2018) (Saini V. et al., 2020) (Islam N. et al., 2022) (McNamara D. et al., 2022) (Mohamed A. et al., 2022)
LE07_L1TP_136045_20101217_20200910_02_T1	Pixel-based method	Built Up Terminal Built Up Infrastructure Built Up Other Depots Built Up Ancillary/Gen. Vegetation/Barren land Forest	$y = 10.9 + 0.0066\ x$	0.15	(The Hazardous […], 2011) (Dip. Tutela Acque, 2022) (Saini V. et al., 2020)
LE07_L1TP_136044_20111204_20200909_02_T1	Pixel-based method	Built Up Terminal Built Up Infrastructure Built Up Other Depots Built Up Ancillary/Gen. Vegetation/Barren land Forest	$y = 10.9 + 0.0066\ x$	0.15	(Saini V. et al., 2020)

LE07_L1TP_136044_20121206_20200908_02_T1	Pixel-based method	Built Up Terminal Built Up Infrastructure Built Up Other Depots Built Up Ancillary/Gen. Vegetation/Barren land Forest	y = -36.6 + 25.9 x	0.93	(Saini V. et al., 2020) (Islam N. et al., 2022)
LC08_L2SP_136045_20131030_20200912_02_T1	Pixel-based method	Built Up Terminal Built Up Infrastructure Built Up Other Depots Built Up Ancillary/Gen. Vegetation/Barren land Forest	y = 44.6 + 0.0101 x	0.273	(Saini V. et al., 2020) (Islam N. et al., 2022)
LC08_L2SP_136044_20141220_20200910_02_T1	Pixel-based method	Built Up Terminal Built Up Infrastructure Built Up Other Depots Built Up Ancillary/Gen. Vegetation/Barren land Forest	y = 1.42 + 0.025 x	0.8	(Rahman A. et al., 2019) (Saini V. et al., 2020) (Islam N. et al., 2022)
LC08_L2SP_136045_20151223_20200908_02_T1	Pixel-based method	Built Up Terminal Built Up Infrastructure Built Up Other Depots Built Up Ancillary/Gen. Vegetation/Barren land Forest	y = 76.8 + 0.009 x	0.058	(Saini V. et al., 2020) (Islam N. et al., 2022)
LC08_L2SP_136045_20161225_20200905_02_T1	Pixel-based method	Built Up Terminal Built Up Infrastructure Built Up Other Depots Built Up Ancillary/Gen. Vegetation/Barren land Forest	y = 34.5 + 0.014 x	0.16	(Saini V. et al., 2020) (Islam N. et al., 2022)
LC08_L1TP_136044_20171126_20200902_02_T1	Pixel-based method	Built Up Terminal Built Up Infrastructure Built Up Other Depots Built Up Ancillary/Gen. Vegetation/Barren land Forest	y = 49.7 + 0.0163 x	0.42	(Rosenfield H., et al., 1986) (Saini V. et al., 2020) (Wang R. et al., 2021) (Islam N. et al., 2022)
LC08_L2SP_136045_20181231_20200830_02_T1	Pixel-based method	Built Up Terminal Built Up Infrastructure Built Up Other Depots Built Up Ancillary/Gen. Vegetation/Barren land Forest	y = 23.3 + 0.0142 x	0.275	(Rahman A. et al., 2019) (Saini V. et al., 2020) (Islam N. et al., 2022)
LC08_L2SP_136045_20191218_20201023_02_T1	Pixel-based method	Built Up Terminal Built Up Infrastructure Built Up Other Depots Built Up Ancillary/Gen. Vegetation/Barren land Forest	y = 0.086 + 0.0138 x	0.66	(Abdullah H. et al., 2013) (Alam S. et al., 2014) (Saini V. et al., 2020) (Islam N. et al., 2022)

Table 5.2 Relationship between Count and Value of Land Use Land Cover per year samples.

Data	Classification method	Cover types	Equation	Linear regression [r^2]	Strategy
LC08_L2SP_136044_20201204_20210313_02_T1	Pixel-based method	Built Up Terminal Built Up Infrastructure Built Up Other Depots Built Up Ancillary/Gen. Vegetation/Barren land Forest	y = 15.9 + 0.0105 x	0.48	(Abdullah H. et al., 2013) (Alam S. et al., 2014) (Saini V. et al., 2020) (Islam N. et al., 2022)
LC09_L2SP_136045_20211215_20220120_02_T1	Pixel-based method	Built Up Terminal Built Up Infrastructure Built Up Other Depots Built Up Ancillary/Gen. Vegetation/Barren land Forest	y = -3,35 + 0,024 x	0.59	(Uddin K. et al., 2003) (Abdullah H. et al., 2013) (Alam S. et al., 2014) (Saini V. et al., 2020) (Dip. Tutela Acque, 2022) (Islam N. et al., 2022)
LC08_L1TP_136044_20220516_20220519_02_T1	Pixel-based method	Built Up Terminal Built Up Infrastructure Built Up Other Depots Built Up Ancillary/Gen. Vegetation/Barren land Forest	y = 14,4 + 0,012 x	0.36	(Abdullah H. et al., 2013) (Alam S. et al., 2014) (Razzaque M. et al., 2019) (Kuveždić D. et al., 2020) (Rahman K. et al., 2021) (Islam N. et al., 2022) (Polverino S., 2022)

LC09_L2SP_136045_20220727_20220729_02_T1	Pixel-based method	Built Up Terminal Built Up Infrastructure Built Up Other Depots Built Up Ancillary/Gen. Vegetation/Barren land Forest	y = 39.2 + 0.03 x	0.35	(Casamonti M., 2006) (Abdullah H. et al., 2013) (Alam S. et al., 2014) (Wadud Z. et al., 2014) (Tran D. et al., 2017) (Kuveždić D. et al., 2020) (Islam N. et al., 2022)

2.3. Root Mean Square Deviation

The Root Mean Square Deviation (RMSD) computed over the LULC values, have indexed the square root of the second sample moment of the differences, occurring amongst predicted values and observed values or the quadratic mean of these differences. The statistical RMSD indicates always non-negative achieved when it comes down to it and it consented to get an initial accuracy of spatial analysis.

$$\mathrm{RMSE} = \sqrt{\sum_{i=1}^{n}(\hat{y}_i - y_i)^2 * {}^{1}/_{n}}$$; whereby $\hat{y}_1, \hat{y}_2, \cdots, \hat{y}_n$ predicted values

$\hat{y}_1, \hat{y}_2, \cdots, \hat{y}_n$ observed values

n number of observations

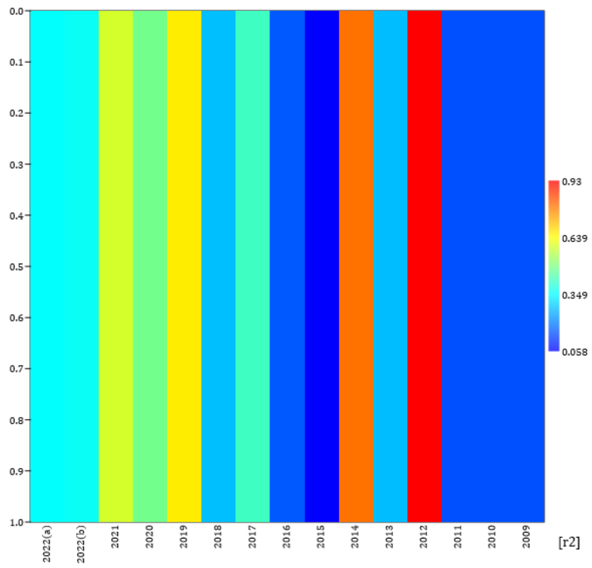

The visual assessment indicates for 2012 the d) class aggregation, interpreted as such for the inaccurate sampling of outer BU Terminal points likewise the non-appearance of the BU Ancillary cover type in some inner and coastal zones.

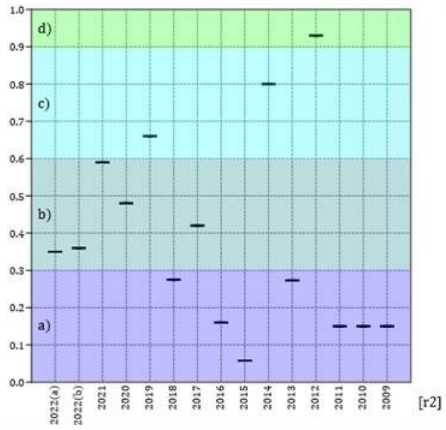

Referenced classes aggregated:

a) 2018, 2016, 2015, 2013, 2011, 2010, 2009; 0.00<a<0.30.
b) 2022(a), 2022(b), 2021, 2020, 2017; 0.30<b<0.60.
c) 2019, 2014; 0.60<c<0.90.
d) 2012; 0.90<d<1.00.

Figure 19-20. Linear regression thresholds and their accountability to the theories of Landscape Architecture.

Table 6.1 Inter-class spectral separability analysis based on similar pixels criteria with regard of the MLE Composite bands classification.

Cover types	Bands	Data	Mean	Std.dev	Data	Mean	Std.dev	Data	Mean	Std.dev	Data	Mean	Std.dev
Built Up Terminal	1	LE07_L1TP_136045_20091214_20200911_02_T1	49.79	3.46	LE07_L1TP_136045_20101217_20200910_02_T1	58.54	3.81	LE07_L1TP_136044_20111204_20200909_02_T1	56.07	1.81	LE07_L1TP_136044_20121206_20200908_02_T1	53.48	3.06
	2		41.86	3.60		52.01	3.96		44.31	1.17		42.41	3.02
	3		45.58	4.73		62.07	6.20		46.49	1.64		47.48	4.72
	4		72.64	2.97		92.06	4.78		78.38	2.15		73.88	4.68
	5		81.45	8.37		125.64	15.29		113.56	10.17		103.51	19.87
	6		132.29	0.93		138.29	1.18		136.67	1.65		138.3	2.10
	7		68.42	8.26		107.98	16.77		109.28	10.51		95.86	20.89
Built Up Infrastructure	1		39.83	6.04		48.37	12.49		50.22	2.66		46.92	2.61
	2		30.03	5.84		39.41	14.18		38.35	2.34		35.89	2.29
	3		28.82	7.23		40.03	19.10		37.42	3.02		35.97	2.93
	4		61.30	11.75		78.21	18.86		68.57	5.84		64.8	6.62
	5		58.46	17.94		79.38	34.47		65.89	14.50		65.21	9.70
	6		131.54	1.88		139.02	3.04		132.49	1.60		134.92	2.08
	7		44.23	15.12		65.83	36.41		53.23	16.92		53.94	8.98

Built Up Other Depots	1	46.15	4.59	51.76	7.99	53.86	1.87	51.08	4.26
	2	36.69	4.73	40.53	7.45	41.67	1.89	39.45	4.62
	3	37.85	6.66	41.07	9.91	40.45	2.66	38.22	6.43
	4	65.50	7.36	74.71	15.18	77.08	5.84	76.62	9.20
	5	71.07	14.72	81.41	27.30	79.99	14.42	76.62	23.53
	6	133.47	2.97	140.06	6.43	132.57	2.25	134.06	3.54
	7	60.19	15.95	75.94	28.17	63.83	18.69	62.54	32.24
Built Up Ancillary/Gen.	1	49.50	5.19	53.31	6.99	51.62	3.28	51.90	3.77
	2	39.73	4.63	42.45	6.58	40.05	2.88	40.10	3.26
	3	41.30	5.43	41.03	9.11	39.01	3.61	38.74	4.45
	4	72.02	10.2	84.12	10.19	70.33	6.80	78.8	8.62
	5	81.03	12.80	75.45	14.07	69.54	12.05	77.45	15.43
	6	133.18	2.78	137.67	3.55	132.80	1.94	133.47	1.92
	7	66.87	14.85	55.98	17.95	55.44	14.38	57.60	17.47
Vegetation/ Barren land	1	41.16	5.54	46.50	6.14	49.79	2.41	48.90	3.63
	2	31.02	4.63	36.17	5.00	38.26	1.96	37.00	2.96
	3	28.81	5.28	33.34	4.91	36.04	2.16	33.69	3.22
	4	65.75	17.16	77.18	22.96	69.32	7.67	78.52	11.45
	5	56.58	16.95	60.16	15.29	59.29	8.69	61.92	10.15
	6	130.73	2.34	137.67	3.92	131.20	1.99	131.50	1.91
	7	39.58	14.11	41.69	13.08	41.42	9.29	40.03	10.09
Forest	1	35.09	3.98	43.07	3.66	47.35	2.13	45.04	2.21
	2	25.22	3.16	31.09	2.90	35.50	1.61	32.84	1.76
	3	21.91	2.93	25.70	2.74	33.10	1.68	28.81	1.83
	4	59.64	11.51	81.56	10.99	66.56	5.84	73.28	6.97
	5	42.04	9.21	49.35	7.16	51.34	11.46	48.61	5.79
	6	129.32	2.09	134.26	2.56	131.15	2.41	130.45	1.54
	7	27.68	7.03	29.26	7.44	36.18	13.04	29.82	5.66

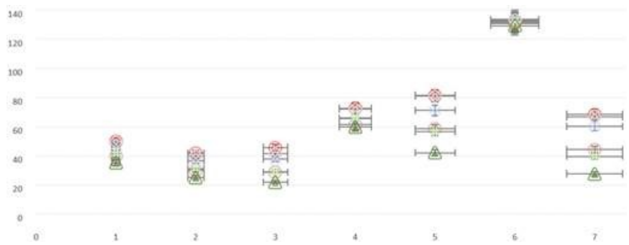
a) LE07_L1TP_136045_20091214_20200911_02_T1

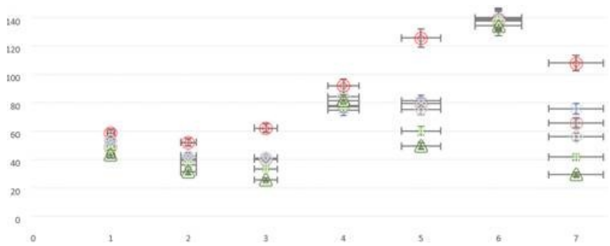
b) LE07_L1TP_136045_20101217_20200910_02_T1

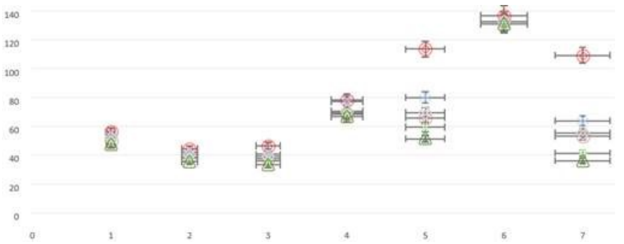
c) LE07_L1TP_136044_20111204_20200909_02_T1

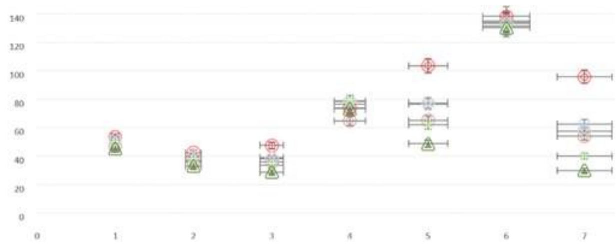
d) LE07_L1TP_136044_20121206_20200908_02_T1

Figure 21.1. a) b) c) d) Mean analysis based on similar pixels criteria. *Referenced symbology

09-12-14[1] 10-12-17[1] 11-12-04[1] 12-12-06[1] 13-10-30[2] 14-12-20[2] 15-12-23[2] 16-12-25[2] 17-11-26[2] 18-12-31[2]

Reference: Landsat-7[1],8[2],9[3]

Table 6.2 Inter-class spectral separability analysis based on similar pixels criteria with regard of the MLE Composite bands classification.

Cover types	Bands	Data	Mean	Std.dev	Data	Mean	Std.dev	Data	Mean	Std.dev	Data	Mean	Std.dev
Built Up Terminal	1	LC08_L2SP_136045_20131030_20200912_02_T1	9,801.85	373.47	LC08_L2SP_136044_20141220_20200910_02_T1	9,291.88	569.44	LC08_L2SP_136045_20151223_20200908_02_T1	9,343.83	371.16	LC08_L2SP_136045_20161225_20200905_02_T1	8,304.07	389.03
	2		8,386.25	481.57		8,552.98	427.26		8,814.33	272.22		8,373.83	243.88
	3		8,692.83	482.66		9,055.04	380.88		9,508.57	279.62		9,080.86	198.36
	4		9,897.75	167.44		9,932.77	73.28		10,559.09	38.16		10,427.17	83.96
	5		11,825.44	1,145.28		10,564.02	613.92		11,502.20	668.79		10,391.72	390.44
	6		14,831.50	1,806.56		11,997.25	1,248.39		14,132.61	1,898.71		10,528.95	1,024.89
	7		14,255.73	1,695.70		11,498.43	1,347.31		13,490.91	1,926.59		9,943.86	1,190.32
Built Up Infrastructure	1		7,765.94	896.22		7,860.45	781.21		7,933,28	488.78		7,837.78	441.34
	2		7,790.03	728.78		7,902.22	599.93		8,196.12	378.27		8,105.71	323.85
	3		8,327.65	642.26		8,478.11	513.87		8,958.37	327.59		8,840.21	282.99
	4		9,561.32	332.35		9,783.37	260.53		10,591.40	151.44		10,418.41	131.57
	5		9,901.12	1,067.47		10,362.26	1,137.62		10,448.89	801.04		10,286.84	955.42
	6		9,758.70	1,154.11		9,994.02	1,239.57		9,840.92	1,266.90		9,752.43	1,283.87
	7		8,912.82	1,061.76		8918.49	1,062.30		8,756.10	1,216.09		8,672.19	1,152.41

Built Up Other Depots	1	8,969.66	1,487.59	7,763.11	940.73	7,270,80	986.77	7,568.20	464.06
	2	8,874.14	1,183.91	7,982.57	856.14	7,761.08	839.00	7,935.43	368.67
	3	9,295.02	908.91	9,056.94	769.06	9,017.87	417.60	9,019.23	375.59
	4	10,181.50	534.64	10,814.67	635.84	11,375.71	380.14	10,995.19	305.47
	5	11,382.10	1,076.67	11,707.63	1,558.57	12,133.49	1,267.96	11,879.78	866.27
	6	11,628.83	1,480.13	12,340.82	2,579.34	13,568.58	2,787.74	13,265.79	2,059.29
	7	11,008.90	1,709.95	11,365.42	2,146.39	12,007.12	2,301.64	12,219.79	1,917.79
Built Up Ancillary/Gen.	1	8,295.38	1,257.61	9,562.23	1,755.99	8,534.96	1,194.26	8,551.32	618.96
	2	8,410.27	1,106.83	9,590.89	1,591.25	8,873.28	1,047.24	8,773.65	511.92
	3	8,825.93	1,032.74	9,989.14	1,435.66	9,590.10	980.71	9,437.93	473.34
	4	9,530.72	386.39	10,390.10	829.01	10,787.80	482.38	10,585.36	221.60
	5	11,397.12	1,418.84	11,936.74	1,266.85	11,497.21	1,112.12	10,743.66	859.50
	6	10,437.07	1,551.78	11,719.44	2,142.24	10,556.59	1,919.83	10,620.68	1,336.92
	7	9,087.21	1,321.66	10,489.47	2,300.91	9,124.83	1,858.45	9,620.69	1,394.55
Vegetation/ Barren land	1	7,376.77	863.23	7,575.50	849.67	7,284.34	656.24	7,378.66	513.95
	2	7,674.79	578.27	7,872.46	589.41	7,883.97	476.85	7,922.12	377.41
	3	8,058.23	522.16	8,344.84	521.56	8,572.90	431.50	8,595.06	357.96
	4	9,236.01	234.59	9,642.39	238.91	10,323.01	213.54	10,275.08	202.23
	5	12,271.47	1,947.23	11,083.47	2,300.84	12,505.61	2,158.72	11,559.17	1,910.25
	6	10,250.71	1,400.16	9,412.01	1,969.26	9,295.00	1,620.94	9,166.77	1,231.73
	7	8,379.59	1,120.48	8,016.53	1,446.35	7,206.35	867.81	7,355.63	744.48
Forest	1	5,890.21	341.72	6,147.37	288.57	6,724.86	162.86	6,707.48	142.03
	2	6,450.82	303.11	6,674.56	245.28	7,370.16	127.59	7,317.48	105.65
	3	7,103.69	283.08	7,395.95	226.52	8,193.20	130.40	8,130.33	103.11
	4	8,961.43	132.89	9,299.04	128.26	10,247.02	96.69	10,121.12	76.59
	5	10,942.01	1,491.18	10,626.55	1,093.58	11,644.72	1,011.91	10,885.99	1,270.65
	6	8,219.16	775.14	8,206.93	672.95	8,441.13	655.25	8,116.61	840.04
	7	6,744.14	545.29	6,808.05	461.03	6,664.47	419.27	6,541.58	475.09

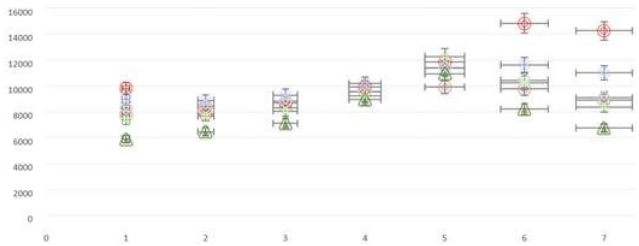

e) LC08_L2SP_136045_20131030_20200912_02_T1

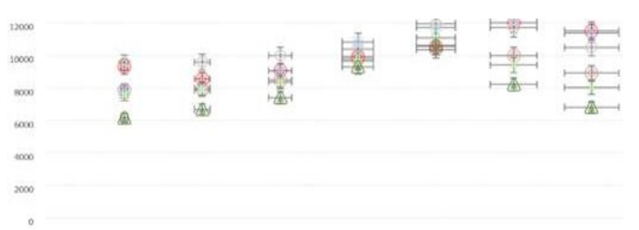

f) LC08_L2SP_136044_20141220_20200910_02_T1

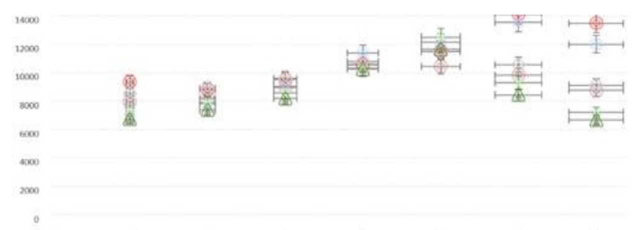

g) LC08_L2SP_136045_20151223_20200908_02_T1

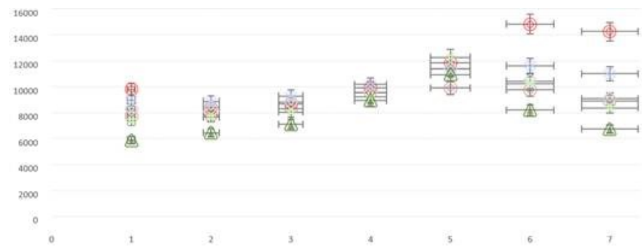

h) LC08_L2SP_136045_20161225_20200905_02_T1

Figure 21.2. e) f) g) h) Mean analysis based on similar pixels criteria. *Referenced symbology

09-12-14[1] 10-12-17[1] 11-12-04[1] 12-12-06[1] 13-10-30[2] 14-12-20[2] 15-12-23[2] 16-12-25[2] 17-11-26[2] 18-12-31[2]

Reference: Landsat-7[1],8[2],9[3]

Table 6.3 Inter-class spectral separability analysis based on similar pixels criteria with regard of the MLE Composite bands classification.

Cover types	Bands	Data	Mean	Std.dev	Data	Mean	Std.dev	Data	Mean	Std.dev	Data	Mean	Std.dev
Built Up Terminal	1	LC08_L1TP_1 36044_20171	9,108.06	718,89	LC08_L2SP_1 36045_20181	8,865.64	525.96	LC08_L2SP_1 36045_20191	483.08	483.08	LC08_L2SP_1 36044_20201	8,443.39	379.82
	2		8,326.71	518.70		8,029.7	527.25		306.64	306.64		8,224.17	251.77
	3		8,877.92	491.91		8,468.56	508.74		272.05	272.05		8,994.49	231.01
	4		10,143.73	115.50		9,595.8	121.49		49.16	49.16		10,504.68	28.09
	5		11,578.14	1,014.18		10,661.84	995.81		813.03	813.03		10,939.00	713.98
	6		13,912.88	2,121.47		12,489.64	1,405.18		1,569.28	1,569.28		12,447.56	1,299.12
	7		13,144.10	2,300.25		1,1852.20	1,413.39		1,638.77	1,638.77		11,916.05	1,471.55

Built Up Infrastructure	1	7,591.00	664.05	7,392.26	594.34	7,573.58	390.56	7,520.44	336.31
	2	7,785.98	485.58	7,439.50	476.34	7,846.05	315.95	7,826.32	264.71
	3	8,521.71	451.65	8,077.62	432.7	8,665.8	292.08	8,685.95	248.22
	4	10,119.21	251.03	9,475.30	176.28	10,442.68	140.13	1,0534.7	116.2
	5	10,446.68	1,021.78	9,284.46	867.47	9,948.7	712.68	9,986.37	661.57
	6	9,955.18	1,366.45	9,180.29	1008.54	9,101.96	867.11	9,206.88	812.46
	7	8,918.59	1,380.51	8,389.78	941.51	8,178.56	826.05	8,263.10	820.69
Built Up Other Depots	1	6,612.78	548.08	6,908.74	635.38	7,700.86	370.11	7,740.43	417.12
	2	7,196.68	565.34	7,420.38	566.06	8,163.26	329.29	8,167.06	356.37
	3	8,820.45	532.01	8,863.16	546.65	9,287.48	369.31	9,222.57	369.34
	4	11,566.44	606.00	11,023.14	793.35	11,204.03	410.82	1,1102.8	315.68
	5	13,086.04	1,101.40	12,409.38	1,308.61	12,286.91	1,055.86	11,910.75	1,059.29
	6	14,930.59	2,289.31	13,444.74	2,501.85	12,538.54	2,364.67	12,319.99	2,443.47
	7	13,313.01	2,063.28	12,483.74	1,867.49	12,018.3	1,749.77	11,905.19	1,878.42
Built Up Ancillary/Gen.	1	8,615.10	1,282.55	9,163.54	1,212.09	8,480.58	881.96	7,985.44	849.07
	2	8,842.09	1,154.54	9,088.47	1,116.88	8,701.04	741.61	8,291.68	719.95
	3	9,399.22	1,098.21	9,448.13	1,050.22	9,383.52	685.12	9,063.37	642.81
	4	10,353.45	595.33	10,004.49	665.31	10,685.12	341.74	10,639.92	245.85
	5	12,009.56	1,374.02	11,430.91	1,364.26	11,517.46	1,253.99	11,217.27	1,167.35
	6	11,163.61	1,601.43	11,377.00	1,722.64	10,909.50	1,510.89	10,526.95	1,522.01
	7	9,739.41	1,607.33	10,122.98	1,579.26	9,706.35	1,510.58	9,349.02	1,597.75
Vegetation/ Barren land	1	6,763.38	580.27	7,139.59	645.08	7,548.43	561.86	7,511.85	481.24
	2	7,459.68	417.37	7,582.01	502.87	8,026.73	411.83	7,979.96	354.89
	3	8,022.02	384.99	8,032.18	441.12	8,733.32	389.68	8,732.32	326.53
	4	9,745.89	225.13	9,333.12	191.02	10,414.3	199.74	10,506.55	165.3
	5	13,725.01	2,849.32	12,013.24	2,228.21	12,054.66	2,092.23	1,1787.8	1,821.97
	6	9,833.86	1,137.78	9,719.39	1,443.02	9,878.72	1,418.55	9,804.85	1,372.58
	7	7,497.82	597.56	7,934.19	950.45	8,057.00	999.22	7,979.29	1,060.12
Forest	1	6,039.36	214.61	5,742.94	230.46	6,583.36	260,34	6,666.14	213.28
	2	6,716.62	171.80	6,325.30	206.37	7,211.11	205.29	7,284.19	167.27
	3	7,487.11	177.69	7,026.29	191.91	8,077.43	207.81	8,180.54	175.77
	4	9,581.04	135.75	9,023.14	245.62	10,207.74	200.46	10,343.17	170.3
	5	12,146.66	1,604.27	10,159.49	1,258.02	11,100.08	1,127.84	11,078.75	1,067.17
	6	8,516.10	624.04	7,924.53	865.65	8,253.20	846.32	8,296.94	787.31
	7	6,673.04	379.75	6,588.96	745.48	6,706.50	742.45	6,689.95	756.88

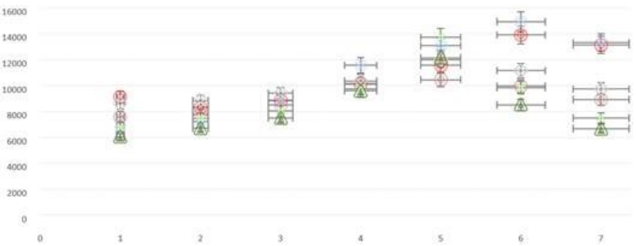

i) LC08_L1TP_136044_20171126_20200902_02_T1

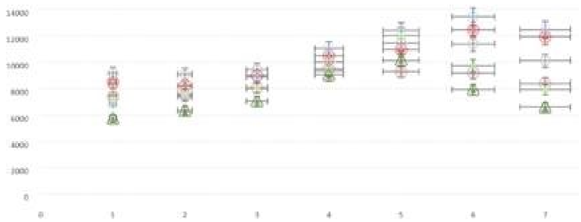

j) LC08_L2SP_136045_20181231_20200830_02_T1

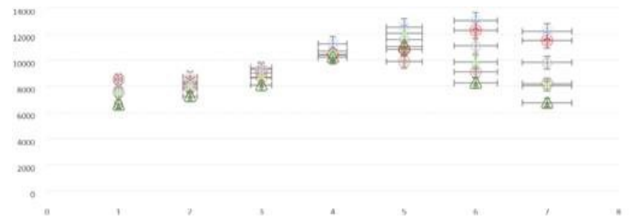

k) LC08_L2SP_136045_20191218_20201023_02_T1

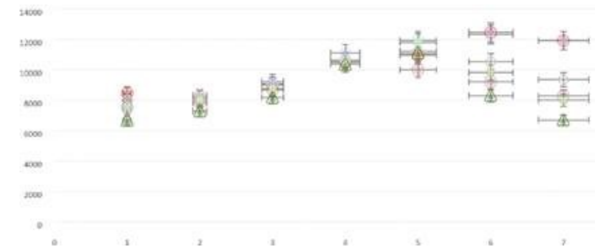

l) LC08_L2SP_136044_20201204_20210313_02_T1

Figure 21.3. i) j) k) l) Mean analysis based on similar pixels criteria. *Referenced symbology

13-10-30[2] 14-12-20[2] 15-12-23[2] 16-12-25[2] 17-11-26[2] 18-12-31[2] 19-12-18[2] 20-12-04[2] 21-12-15[3] 22-05-16[3]

Reference: Landsat-7[1],8[2],9[3]

Table 6.4 Inter-class spectral separability analysis based on similar pixels criteria with regard of the MLE Composite bands classification.

Cover types	Bands	Data	Mean	Std.dev	Data	Mean	Std.dev	Data	Mean	Std.dev	Data	Mean	Std.dev
Built Up Terminal	1	LC09_L2SP_136045_20211	9,243.24	533.42	LC08_L1TP_136044_20220	8,608.79	438.14	LC09_L2SP_136045_20220	12,025.97	1,294.09	NO DATA	NO DATA	NO DATA
	2		8,640.20	277.15		8,345.53	201.7		11,416.92	1,034.82		NO DATA	NO DATA
	3		9,311.91	244.6		9,106.43	196.86		11,927.08	880.43		NO DATA	NO DATA
	4		10,513.84	59.55		10,451.47	42.59		12,917.42	596.88		NO DATA	NO DATA
	5		11,427.51	902.49		10,641.92	551.59		14,240.47	1,622.74		NO DATA	NO DATA
	6		13,312.53	1,845.17		12,028.19	1,695.18		14,525.53	3,307.2		NO DATA	NO DATA
	7		12,328.04	1,672.39		11,411.58	1,694.29		12,437.25	2,808.51		NO DATA	NO DATA

Built Up Infrastructure	1	7,581.01	362.78	7,653.88	365.36	9,207.42	1,244.94	NO DATA	NO DATA
	2	7,826.21	288.81	7,923.75	296.29	9,412.35	943.98	NO DATA	NO DATA
	3	8,650.08	268.35	8,720.69	249.13	10,088.16	868.51	NO DATA	NO DATA
	4	10,422.51	115.33	10,453.04	103.24	11,826.78	494.68	NO DATA	NO DATA
	5	9,996.86	553.80	10,109.68	841.49	14,153.51	2,249.51	NO DATA	NO DATA
	6	9,386.42	626.60	9,351.31	1,185.84	12,603.32	1,520.43	NO DATA	NO DATA
	7	8,344.60	607.41	8,341.26	951.00	10,292.27	1,419.60	NO DATA	NO DATA
Built Up Other Depots	1	7,518.35	694	7,489.45	584.22	8,708.48	1,656.82	NO DATA	NO DATA
	2	8,116.30	659.24	7,992.85	540.56	9,716.28	1,717.56	NO DATA	NO DATA
	3	9,494.87	579.71	9,256.37	489.84	11,657.12	2,038.45	NO DATA	NO DATA
	4	11,684.18	590.89	11,364.99	413.62	14,646.42	2,186.00	NO DATA	NO DATA
	5	13,294.57	1,388.67	12,458.43	1,026.92	18,023.78	4,573.60	NO DATA	NO DATA
	6	14,692.90	3,301.83	13,350.07	2,383.73	18,581.55	6,392.45	NO DATA	NO DATA
	7	13,124.92	2,303.25	12,135.11	1,870.33	16,500.74	5,739.54	NO DATA	NO DATA
Built Up Ancillary/Gen.	1	8,905.74	954.39	8,990.89	950.45	9,478.47	3,222.40	NO DATA	NO DATA
	2	9,039.01	825.47	9,087.74	833.56	9,940.63	2,867.39	NO DATA	NO DATA
	3	9,665.44	795.68	9,706.25	792.44	10,504.16	2,671.42	NO DATA	NO DATA
	4	10,774.96	355.02	10,812.29	341.78	11,984.86	1,712.13	NO DATA	NO DATA
	5	11,653.34	1,308.32	11,559.57	1,208.71	15,959.99	4,051.85	NO DATA	NO DATA
	6	11,448.03	1,454.99	11,215.84	1,305.18	13,037.57	3,437.29	NO DATA	NO DATA
	7	10,058.09	1,313.52	9,971.57	1,291.19	10,396.38	3,194.07	NO DATA	NO DATA
Vegetation/ Barren land	1	7,320.24	598.34	7318.81	551.43	7,779.52	1,230.43	NO DATA	NO DATA
	2	7,927.82	418.94	7888.06	412.13	8,780.85	981.42	NO DATA	NO DATA
	3	8,584.24	421.67	8582.30	391.37	9,241.42	879.27	NO DATA	NO DATA
	4	10,328.32	255.22	10345.85	223.49	11,312.35	589.85	NO DATA	NO DATA
	5	12,520.72	2,728.54	12280.79	2,129.34	17,914.24	5,503.53	NO DATA	NO DATA
	6	9,571.68	1,234.56	9568.39	1,212.70	11,575.09	2,357.34	NO DATA	NO DATA
	7	7,447.64	610.72	7590.80	735.83	8,368.23	1,320.36	NO DATA	NO DATA
Forest	1	6,386.29	199.77	6,600.10	248.90	6,626.82	1,015.42	NO DATA	NO DATA
	2	7,098.52	166.49	7,240.54	195.45	7,697.20	927.41	NO DATA	NO DATA
	3	7,938.61	179.64	8,096.59	194.80	8,392.51	888.35	NO DATA	NO DATA
	4	10,106.72	142.91	10,198.97	145.64	10,843.04	515.59	NO DATA	NO DATA
	5	12,294.51	1,514.40	11,230.37	1182.78	17,955.92	4,089.51	NO DATA	NO DATA
	6	8,738.12	726.68	8,208.47	662.65	11,211.65	2,148.59	NO DATA	NO DATA
	7	6,694.35	384.93	6,609.77	447.07	7,929.65	1,484.54	NO DATA	NO DATA

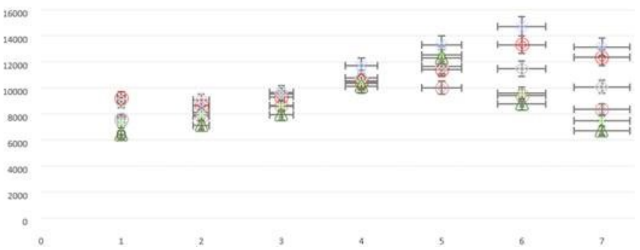

m) LC09_L2SP_136045_20211215_20220120_02_T1

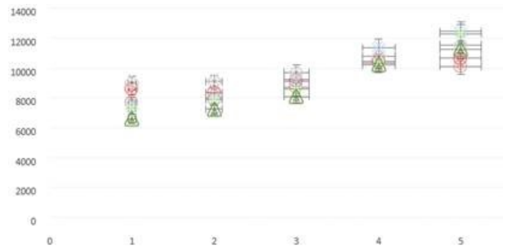

n) LC08_L1TP_136044_20220516_20220519_02_T1

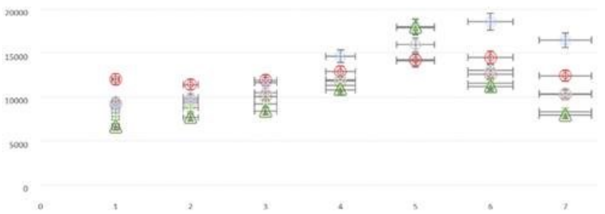

o) LC09_L2SP_136045_20220727_20220729_02_T1

Figure 21.4. m) n) o) Mean analysis based on similar pixels criteria. *Referenced symbology

14-12-20[2]	15-12-23[2]	16-12-25[2]	17-11-26[2]	18-12-31[2]	19-12-18[2]	20-12-04[2]	21-12-15[3]	22-05-16[3]	22-07-27[3]

Reference: Landsat-7[1],8[2],9[3]

Table 7.1 OLI Landsat 7-8 mosaic datasets in accordance with an pixel-based method.

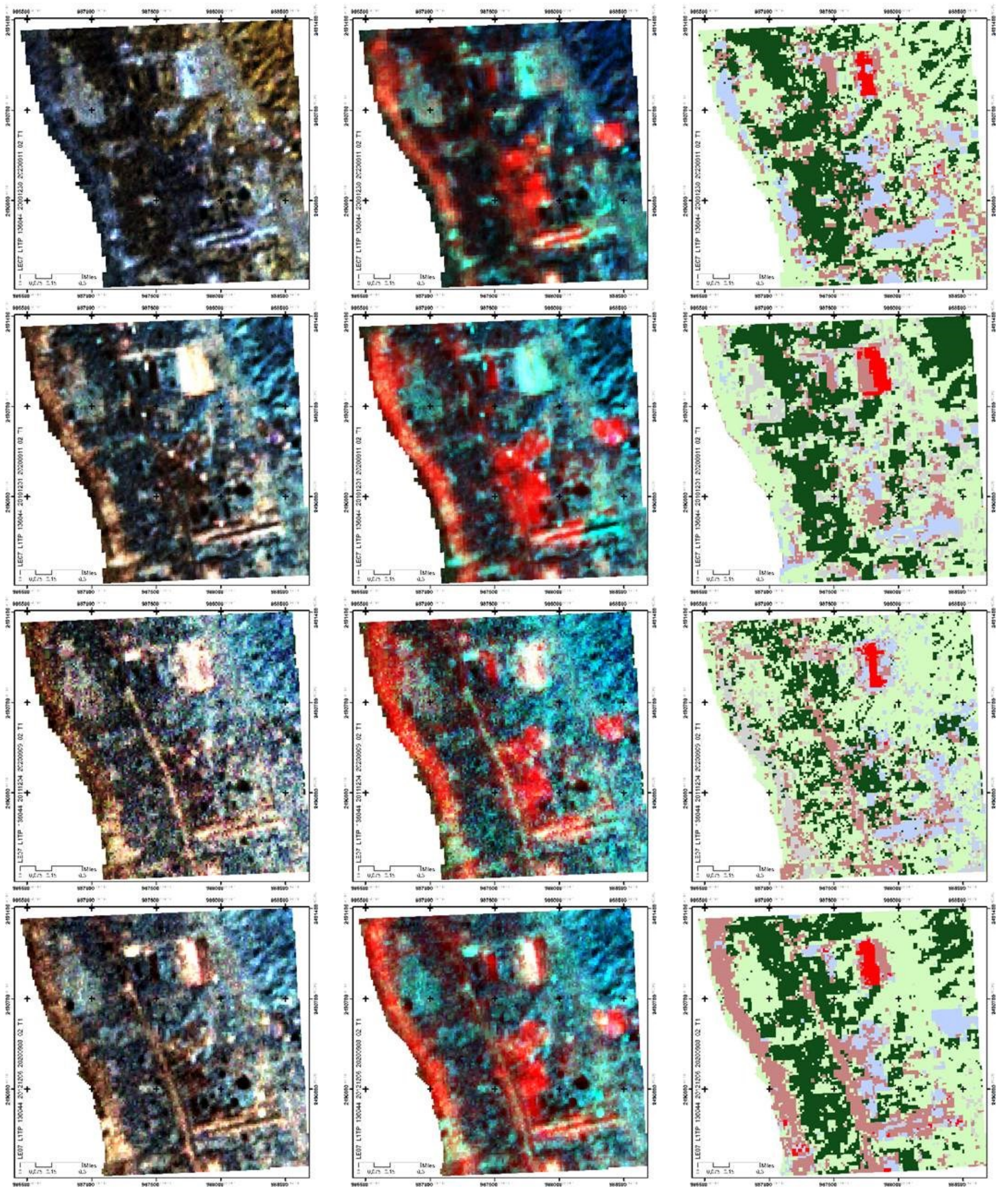

09-12-14[1]	10-12-17[1]	11-12-04[1]	12-12-06[1]	13-10-30[2]	14-12-20[2]	15-12-23[2]	16-12-25[2]	17-11-26[2]	18-12-31[2]

Reference: Landsat-7[1],8[2],9[3]

Table 7.2 OLI Landsat 8 mosaic datasets in accordance with an pixel-based method.

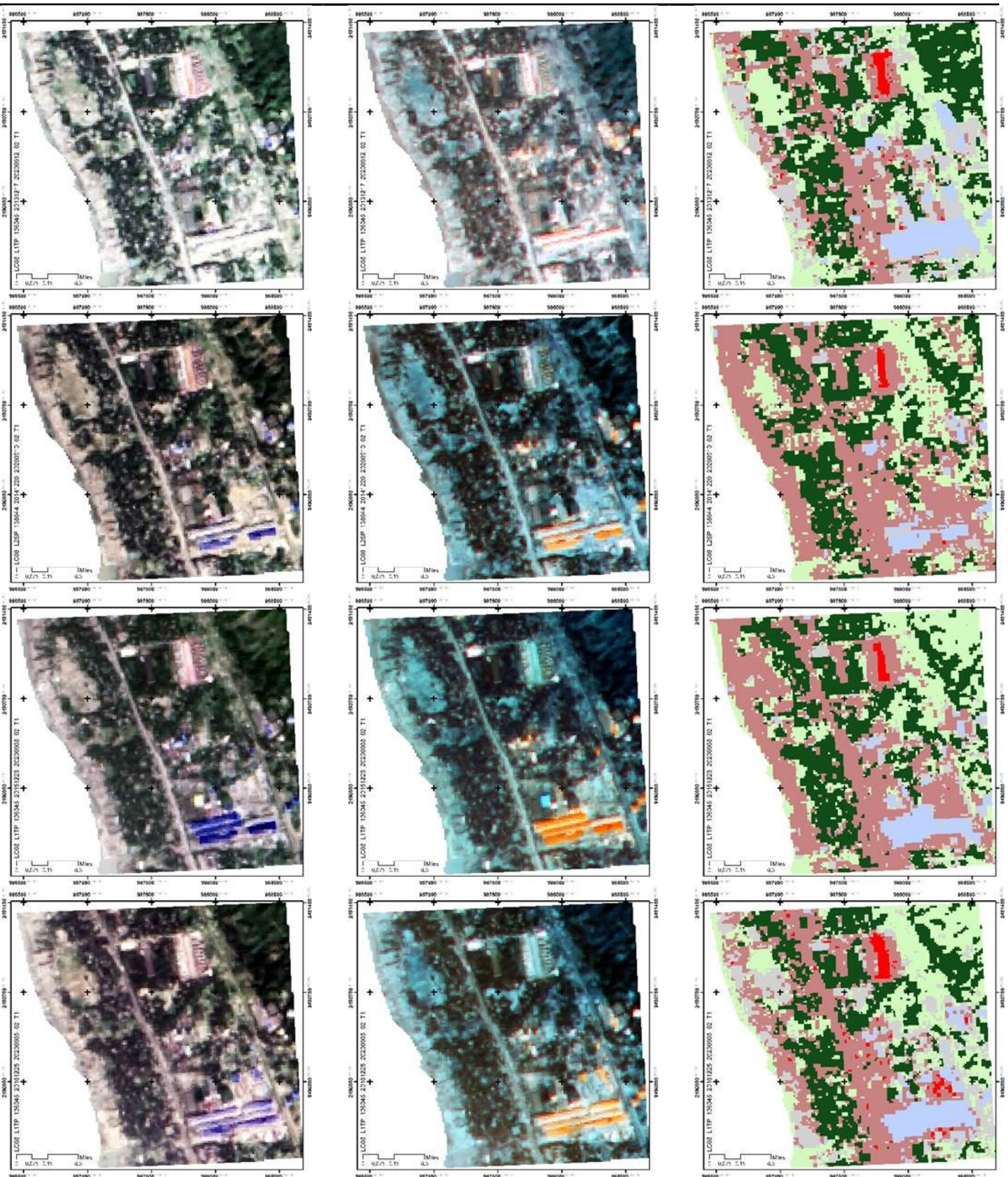

09-12-14[1]	10-12-17[1]	11-12-04[1]	12-12-06[1]	13-10-30[2]	14-12-20[2]	15-12-23[2]	16-12-25[2]	17-11-26[2]	18-12-31[2]

Reference: Landsat-7[1],8[2],9[3]

Table 7.3 OLI Landsat 8 mosaic datasets in accordance with an pixelt-based method.

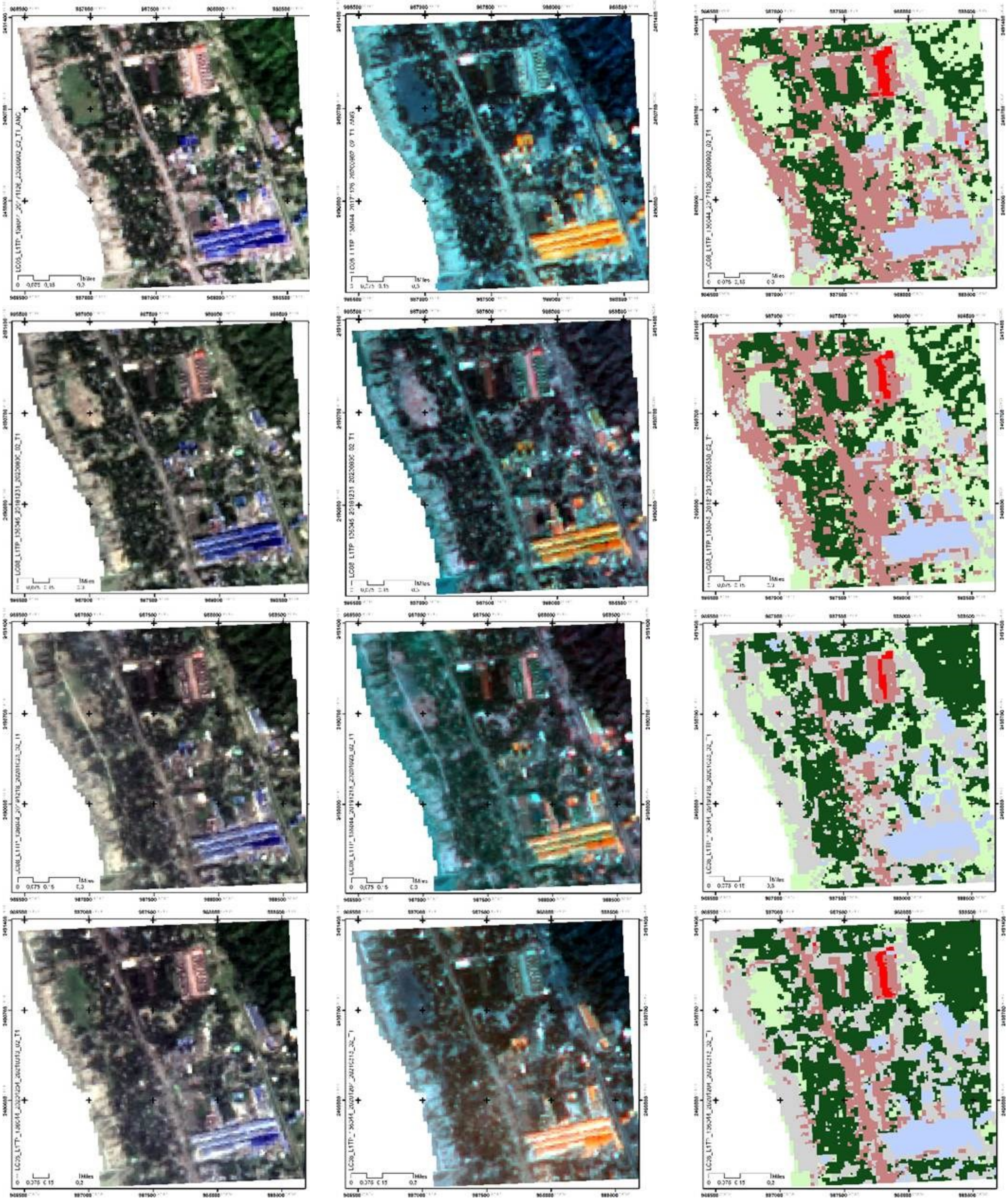

13-10-30[2]	14-12-20[2]	15-12-23[2]	16-12-25[2]	17-11-26[2]	18-12-31[2]	19-12-18[2]	20-12-04[2]	21-12-15[3]	22-05-16[3]

Reference: Landsat-7[1],8[2],9[3]

Table 7.4 OLI Landsat 8 mosaic datasets in accordance with an pixel-based method.

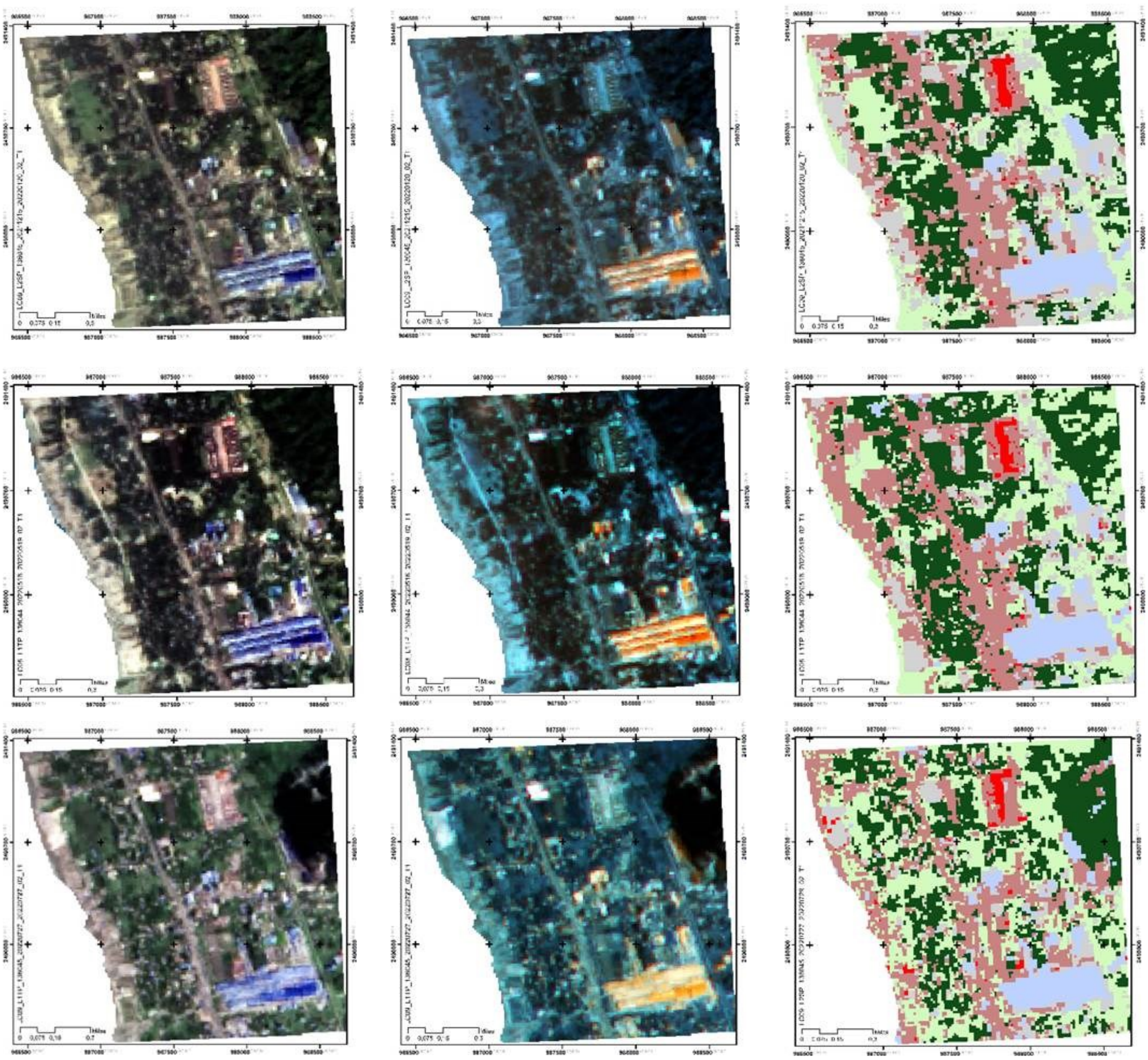

14-12-20[2]	15-12-23[2]	16-12-25[2]	17-11-26[2]	18-12-31[2]	19-12-18[2]	20-12-04[2]	21-12-15[3]	22-05-16[3]	22-07-27[3]

Reference: Landsat-7[1],8[2],9[3]

2.4. Accuracy kappa

According to a stratified bibliography over Kappa indices of agreement (Aickin M., 1990, Byrt T. et al., 1993, Brennan R. et al., 1981, Cohen J., 1960, 1968, Fleiss J. et al., 1969, Hudson W. D. et al., 1987), during the early stage-framework, we researched the current improvement of its Kappa Coefficient, starting from the premises of a critical witness of certain scientific articles (Pontius R. G. et al., 2011) which underline the implicit K limitations; nonetheless K statistics remains, a commonly accepted statistical-thematic mapping (Olofsson P. et al., 2013), and despite of its cited deprecability, we moved to propose a consistent temporal variance of those classifications versus agreement due to random chance: 1) random distribution of the quantity of each category, and 2) random spatial allocation of the categories. Three fundamental steps demanded us to take a firm position with regard of: 1) a proper picking of certain urban thematic cover types, according to the LA theories already acknowledged and those not yet investigated (Landis J. et al., 1977); 2) gathering a high volume of data, so that the initial premises of final Infrastructure change, would have been respected; consequently the remote-sensed urban investigation is considered as a practical set of applications to the exercise of the profession, without being accounted as a self-referential urban-regeneration project; 3) plotting and analysing the cross labelled results, in agreement with multicriterial -scalar parameters. The study has thus accounted a stratified random sample, part of the multinomial sampling methods, by which we indeed accounted fundamental issues, i.e.: (1) which points must be stratified by map category; (2) how to increment quantitively each stratum referring to simple random samplings at once (Stehman S. V. et al., 2019). As rigorously planned, the volume also indicates Kappa distribution across the landscape (Türk G., 1979), so the auxiliary recommendations were included in the decisional process, as: 1) which type of raster combination to start with; 2) the appropriate sampling unit; 3) how many examples to be taken; 4) which would it be the reference ground-truth map to assess the producer percentages. The hierarchy is determined by the dependency of sampling design towards the amount of sample points. In the criteria of a sampling design, the minimum level of accuracy has a significant role in terms of reference pixels for which the scarcity of a weak assigned distribution is a result of inconvenient equations to be nominated.

$$N = 4(p)(q')/E^2$$

whereby:

N = total number of points to be sampled
P = projected percent accuracy
$q' = 100 - p$
E = admissible accuracy

Equation 1. Classification equation. Model number of pixels to sample as reference points for an overall accuracy assessment.

$$PCC = \frac{S_d}{\mathrm{n}} \ 100\ \%$$

Equation 2. Attribute data accuracy. The equation relies on three indices as follows.

$$S_d = summation\ of\ values\ along\ diagonal$$
$$n = total\ number\ of\ sample\ location$$

Equation 3. Overall Accuracy (Percentage Correctly Classified).

$$PCC = \frac{C_i}{C_t} \ 100\ \%$$
$$C_i = properly\ classified\ sample\ location\ in\ column$$
$$C_t = global\ number\ of\ sample\ location\ in\ column$$

Equation 4. Producers Accuracy. Global number of properly classified pixels depending on each category, is divided by the global number of pixels consisting that category.

$$UA = \frac{R_i}{R_t} \ 100\ \%$$

$$R_i = properly\ classify\ sample\ location\ in\ row$$
$$R_t = global\ number\ of\ sample\ location\ in\ row$$
$$\mathrm{EOC} = 100 - user'saccuracy$$
The omission error is 1 – producer's accuracy;
The commission error is 1 – user's accuracy.

Equation 5. User's Accuracy benchmarks a specific category assuming that probability of classification, for each spatial data unit, transferred to that particular category on ground. EOC is measured according to this accuracy criteria.

2.2.4.5.5.1 Kappa Coefficient

Based on international research, one established on kappa measurement, starting on the premises of the difference between the agreements, occurring between two maps, in the matter of the diagonal entries in the error matrix.

The literature existing on such measurement, also has appreciated its versatility in order to compare numerically and statistically two classification products thanks to: (1) the implementation of an algorithm multiple-choice, (2) the non-entailment of different reference data for validation.

$$K = P_0 - P_c \ /\ 1 - P_c$$
$$P_0 = \sum_{i=1}^{m} P_{ii} = 1\ /\ N \sum_{i=1}^{m} N_{ii}$$
$$P_c = \sum_{i=1}^{m} P_i + P + I = 1\ /\ N2 \sum_{i=1}^{m} N_i + N + I$$
$$N_i + N + I = A + B + C + D + E + F = 269$$

$$K = 0.5714 - 0.2196\ /\ 1 - 0.2196 = 0.451$$

$$K = P_0 - P_c \ /\ 1 - P_c$$

Equation 6. The goal of Kappa coefficient is indeed to measure the agreement between two systems. In remote sensing, one applies this to define and partially to compensate the classification precision of algorithm comparing the output of algorithm with already classified image/dataset (waiting result). The strongest Kappa, hence, identifies the most precise algorithm, however, this case is true, if the classified categories rely on similar cases. Kappa considers all categories as equal sets (that normalize the number of samples).

Table 8.1 Classification accuracy employing OLI Landsat 8 datasets in accordance with an object-based method.

Data	Classification method	Cover types	Producer accuracy (%)	User accuracy (%)	Total classification accuracy (%)	Kappa coefficient (%)
LE07_L1TP_136045_20091214_20200911_02_T1	Object-based method	Built Up Terminal	0.00	0.00	62.06	47.59
		Built Up Infrastructure	61.11	45.83		
		Built Up Other Depots	92.85	65.00		
		Built Up Ancillary/Gen.	0.00	0.00		
		Vegetation/Barren land	53.44	70.45		
		Forest	68.00	94.44		
LE07_L1TP_136045_20101217_20200910_02_T1	Object-based method	Built Up Terminal	83.33	33.33	69.82	61.19
		Built Up Infrastructure	70.58	80.00		
		Built Up Other Depots	80.00	80.00		
		Built Up Ancillary/Gen.	63.63	46.66		
		Vegetation/Barren land	63.82	76.92		
		Forest	76.00	86.36		
LE07_L1TP_136044_20111204_20200909_02_T1	Object-based method	Built Up Terminal	100.00	46.15	65.21	54.57
		Built Up Infrastructure	66.66	76.19		
		Built Up Other Depots	75.00	66.66		
		Built Up Ancillary/Gen.	72.72	53.33		
		Vegetation/Barren land	59.61	79.48		
		Forest	57.14	44.44		
LE07_L1TP_136044_20121206_20200908_02_T1	Object-based method	Built Up Terminal	100.00	61.53	68.37	58.61
		Built Up Infrastructure	68.57	77.41		
		Built Up Other Depots	61.53	72.72		
		Built Up Ancillary/Gen.	50.00	33.33		
		Vegetation/Barren land	72.22	63.41		
		Forest	56.52	72.22		
LC08_L2SP_136045_20131030_20200912_02_T1	Object-based method	Built Up Terminal	100.00	85.71	70.53	63.20
		Built Up Infrastructure	91.66	89.18		
		Built Up Other Depots	100.00	46.66		
		Built Up Ancillary/Gen.	45.45	22.72		
		Vegetation/Barren land	30.00	75.00		
		Forest	86.36	100.00		
LC08_L2SP_136044_20141220_20200910_02_T1	Object-based method	Built Up Terminal	83.33	100.00	90.43	86.98
		Built Up Infrastructure	100.00	81.48		
		Built Up Other Depots	100.00	100.00		
		Built Up Ancillary/Gen.	71.42	100.00		
		Vegetation/Barren land	73.07	95.00		
		Forest	100.00	100.00		
LC08_L1TP_136045_20151223_20200908_02_T1	Object-based method	Built Up Terminal	62.50	100.00	80.87	74.61
		Built Up Infrastructure	92.68	71.69		
		Built Up Other Depots	100.00	90.90		
		Built Up Ancillary/Gen.	55.55	55.55		
		Vegetation/Barren land	56.00	100.00		
		Forest	95.45	91.30		
LC08_L2SP_136045_20161225_20200905_02_T1	Object-based method	Built Up Terminal	100.00	60.00	73.68	67.59
		Built Up Infrastructure	82.14	69.69		
		Built Up Other Depots	85.71	92.30		
		Built Up Ancillary/Gen.	52.17	54.54		
		Vegetation/Barren land	58.33	82.35		
		Forest	89.47	89.47		
LC08_L1TP_136044_20171126_20200902_02_T1	Object-based method	Built Up Terminal	100.00	90.90	84.61	81.10
		Built Up Infrastructure	100.00	73.68		
		Built Up Other Depots	92.85	100.00		
		Built Up Ancillary/Gen.	63.63	87.50		
		Vegetation/Barren land	85.71	78.26		
		Forest	72.72	100.00		

09-12-14[1]	10-12-17[1]	11-12-04[1]	12-12-06[1]	13-10-30[2]	14-12-20[2]	15-12-23[2]	16-12-25[2]	17-11-26[2]	18-12-31[2]

Reference: Landsat-7[1],8[2],9[3]

Table 8.2 Classification accuracy employing OLI Landsat 8 datasets in accordance with an object-based method.

Data	Classification method	Cover types	Producer accuracy (%)	User accuracy (%)	Total classification accuracy (%)	Kappa coefficient (%)
LC08_L2SP_136045_20181231_20200830_02_T1	Object-based method	Built Up Terminal	100.00	100.00	89.74	87.17
		Built Up Infrastructure	100.00	94.60		
		Built Up Other Depots	100.00	100.00		
		Built Up Ancillary/Gen.	88.88	61.53		
		Vegetation/Barren land	68.00	85.00		
		Forest	86.95	90.90		
LC08_L2SP_136045_20191218_20201023_02_T1	Object-based method	Built Up Terminal	90.00	90.00	77,77	73.06
		Built Up Infrastructure	88.88	72.72		
		Built Up Other Depots	94.11	94.11		
		Built Up Ancillary/Gen.	72.00	62.06		
		Vegetation/Barren land	48.14	86.66		
		Forest	95.00	79.16		
LC08_L2SP_136044_20201204_20210313_02_T1	Object-based method	Built Up Terminal	90.00	90.00	76.92	72.01
		Built Up Infrastructure	81.25	68.42		
		Built Up Other Depots	94.11	94.11		
		Built Up Ancillary/Gen.	79.16	59.37		
		Vegetation/Barren land	46.66	81.25		
		Forest	95.00	82.60		
LC09_L2SP_136045_20211215_20220120_02_T1	Object-based method	Built Up Terminal	80.00	88.88	91.37	89.42
		Built Up Infrastructure	96.66	93.54		
		Built Up Other Depots	100.00	100.00		
		Built Up Ancillary/Gen.	90.90	58.82		
		Vegetation/Barren land	79.16	100.00		
		Forest	95.65	100.00		
LC08_L1TP_136044_20220516_20220519_02_T1	Object-based method	Built Up Terminal	100.00	90.90	88.33	85.52
		Built Up Infrastructure	86.48	86.48		
		Built Up Other Depots	100.00	100.00		
		Built Up Ancillary/Gen.	85.71	63.15		
		Vegetation/Barren land	80.00	94.11		
		Forest	86.36	100.00		
LC09_L2SP_136045_20220727_20220729_02_T1	Object-based method	Built Up Terminal	88.88	88.88	95.68	94.54
		Built Up Infrastructure	100.00	94.73		
		Built Up Other Depots	100.00	100.00		
		Built Up Ancillary/Gen.	66.66	100.00		
		Vegetation/Barren land	95.83	95.83		
		Forest	95.83	95.23		

14-12-20[2]	15-12-23[2]	16-12-25[2]	17-11-26[2]	18-12-31[2]	19-12-18[2]	20-12-04[2]	21-12-15[3]	22-05-16[3]	22-07-27[3]

Reference: Landsat-7[1],8[2],9[3]

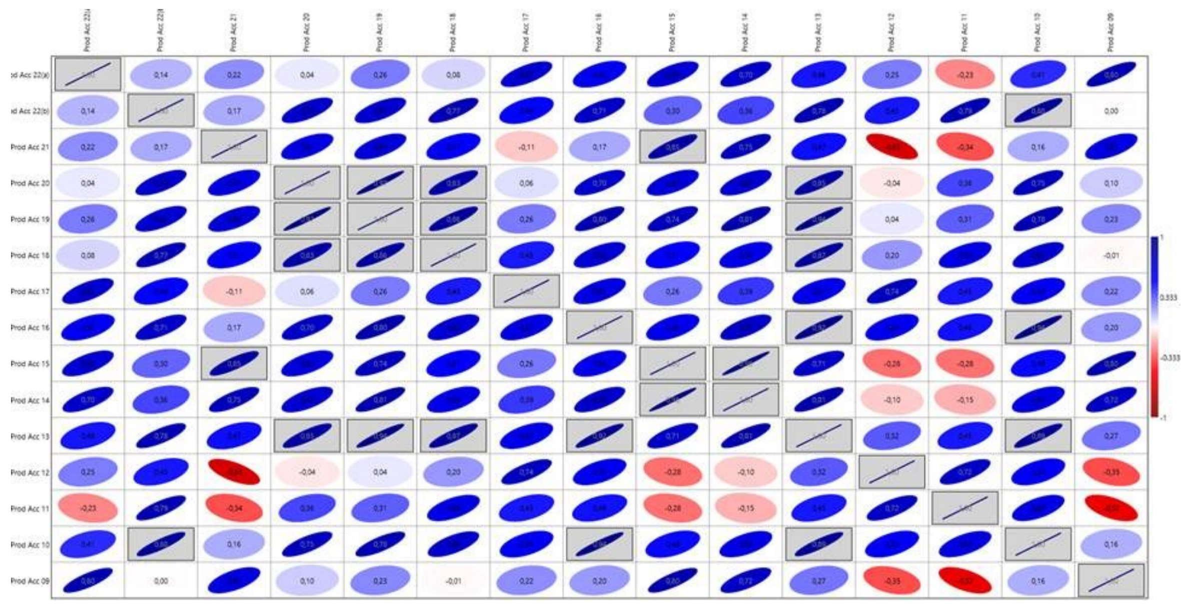

Figure 22. Pearson correlation across Producer values, yearly based. 21-12, 11-09, 09-11 represent the blandest linear bivariation.

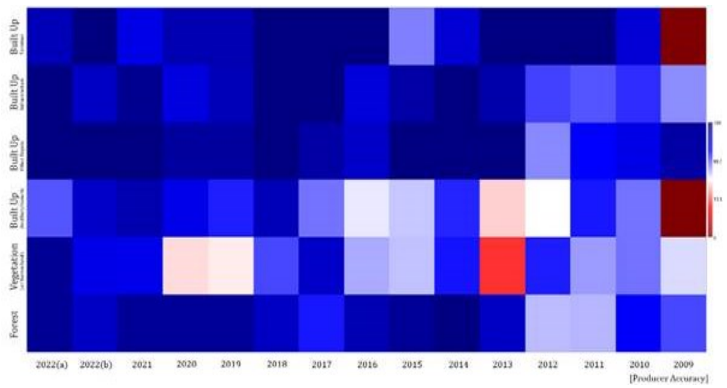

Figure 23. Producer accuracy correspondence matrix correlated. BM Terminal construction stage has performed the lowest percentage value over the set.

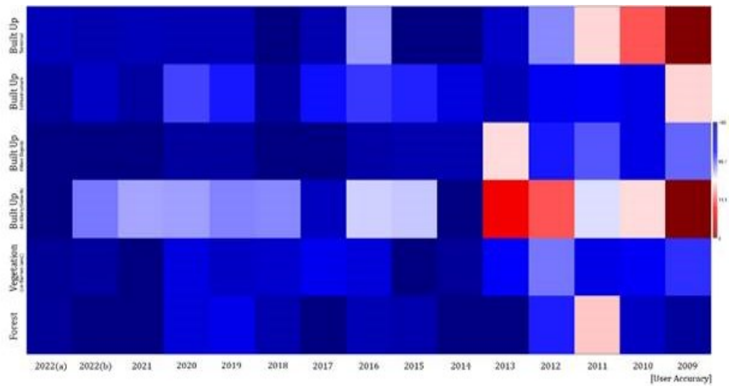

Figure 24. An important inconsistency is accounted for built-up classifications in the a) area. This discrepancy might be depending on the result of the dominant class and restrictions in the training data samples.

Figure 25. BM Terminal. 04/2009 (*et similia).

Figure 26. BM Terminal. 03/2011.

Figure 27. BM Terminal. 01/2012.

Figure 28. BM Terminal. 01/2013.

Figure 29. BM Terminal. 10/2014.

Figure 30. BM Terminal. 10/2014.

Figure 31. BM Terminal. 11/2014.

Figure 32. BM Terminal. 11/2015.

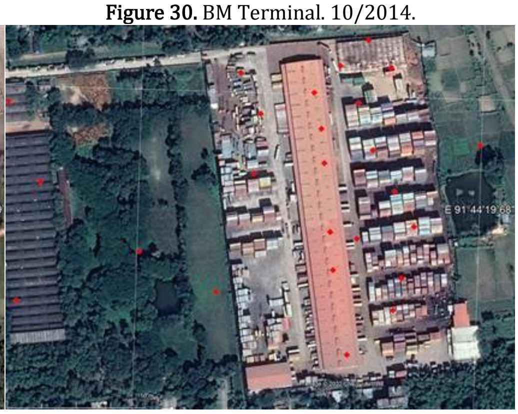

Figure 33. BM Terminal. 11/2016.

*Google uses its own custom projection.

Figure 34. BM Terminal. 06/2017 (*et similia).

Figure 35. BM Terminal. 12/2018.

Figure 36. BM Terminal. 11/2019.

Figure 37. BM Terminal. 11/2020.

Figure 38. BM Terminal. 12/2021.

Figure 39. Steel Industry. 04/2009.

Figure 40. Steel Industry. 03/2011.

Figure 41. Steel Industry. 01/2012.

Figure 42. Steel Industry. 12/2013.

Figure 43. Steel Industry. 10/2015.

Figure 44. Steel Industry. 10/2016.

Figure 45. Coastal sampling 01. 04/2009.

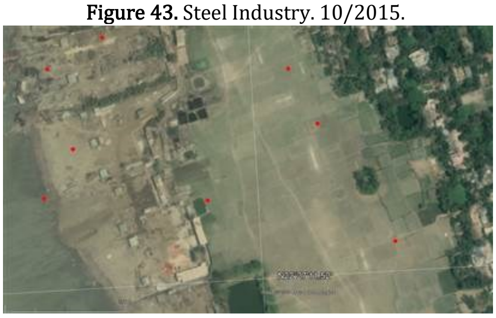

Figure 46. Coastal sampling 01. 03/2011.

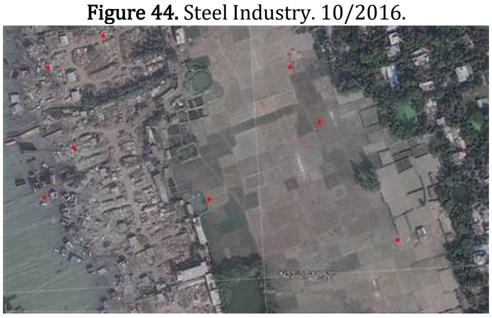

Figure 47. Coastal sampling 01. 01/2013.

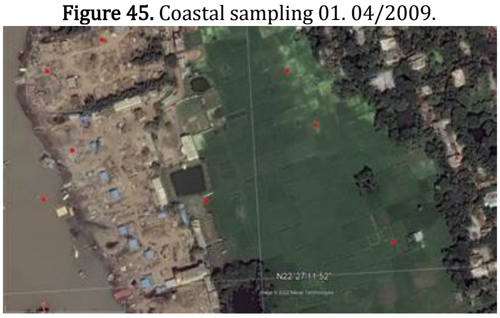

Figure 48. Coastal sampling 01. 10/2016.

*Google uses its own custom projection.

Figure 49. Coastal sampling 02. 04/2009 (*et sim.).

Figure 50. Coastal sampling 02. 03/2011.

Figure 51. Coastal sampling 02. 10/2016.

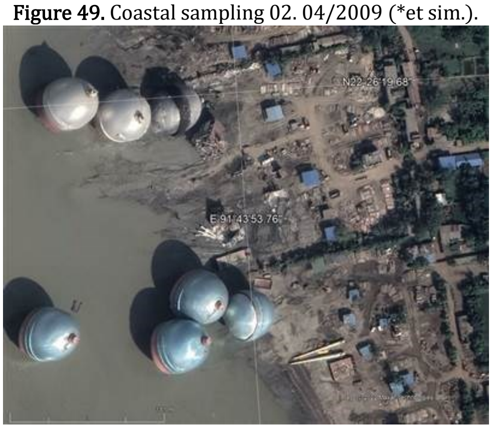

Figure 52. Coastal sampling 02. 12/2019.

Figure 53. Power Station. 04/2009.

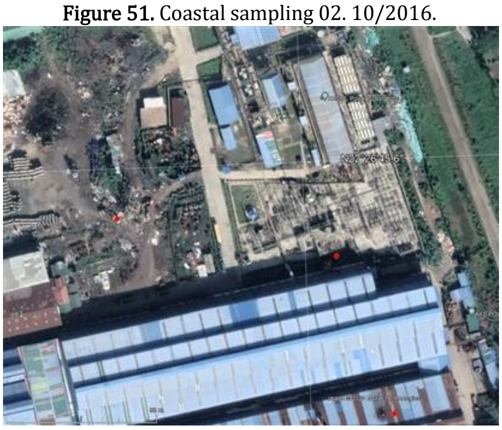

Figure 54. Power Station. 12/2021.

*Google uses its own custom projection.

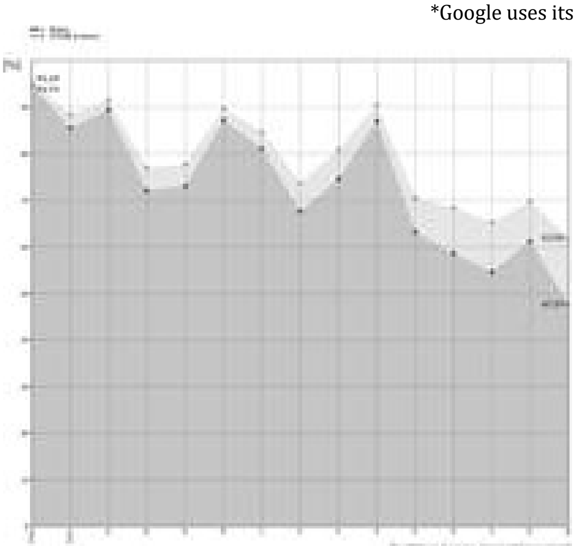

Figure 55. Kappa-OA accuracy pairing.

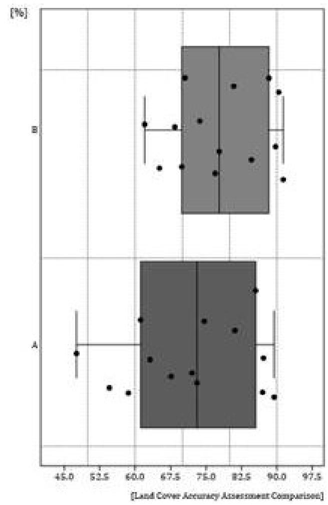

Figure 56. Bar chart with median factors: 74.61 % (A), 77.77 % (B).

2.5. Annual change rate

The vegetative/barren land decreased constantly, partially depending on inland fishery, followed by MLE indication of the infrastructural cover type, determined by the allocation of its equipment, so that the shores became temporarily occupied with infrastructural and generic built-up cover category land.

The intrusion of monsoon did not significantly impact on the industrial sector, so that we comprehend across the Producer and User indexation, overall higher values, in constant margins, included in the a) class.

The visual natural barrier mangroves, disrupted by the local inhabitants together with the release of toxic waters, derived from the heavy industries, so that this systemic driver is decreasing, year by year. Roads and other minor paths of communication have been all clearly computed in a distinguishable way and do not manifest alterations.

Table 9.1 Classification areal percentage employing OLI Landsat 8 datasets in accordance with an object-based method.

Data	Classification method	Cover types	Index (%a)	Area (mq)	Change year (%b)	Annual change rate (%c)		
LE07_L1TP_136045_20091214_20200911_02_T1	Object-based method	Built Up Terminal	1.04	38,476.18	N/A	N/A	N/A	N/A
		Built Up Infrastructure	14.68	539,103.73				
		Built Up Other Depots	10.55	387,423.52				
		Built Up Ancillary/Gen.	0.55	20,411.00				
		Vegetation/Barren land	44.58	1,636,893.23				
		Forest	28.57	1,049,145.62				
LE07_L1TP_136045_20101217_20200910_02_T1	Object-based method	Built Up Terminal	1.33	49,056.64	24.59	24.60	N/A	N/A
		Built Up Infrastructure	8.87	325,961.85	-50.38	-50.38		
		Built Up Other Depots	5.00	183,334.18	-74.66	-74.66		
		Built Up Ancillary/Gen.	13.42	493,057.78	-22.55	319.45		
		Vegetation/Barren land	38.48	1,412,859.00	-14.71	-14.71		
		Forest	32.88	1,207,475.41	14.05	14.05		
LE07_L1TP_136044_20111204_20200909_02_T1	Object-based method	Built Up Terminal	0.95	34,895.16	-33.64	-4.50	N/A	N/A
		Built Up Infrastructure	12.64	464,308.62	35.41	-7.48		
		Built Up Other Depots	7.24	266,152.23	37.01	-18.82		
		Built Up Ancillary/Gen.	10.71	393,580.31	-127.89	148.45		
		Vegetation/Barren land	49.00	1,798,890.27	-14.37	4.72		
		Forest	19.43	713,683.37	-52.60	-20.27		
LE07_L1TP_136044_20121206_20200908_02_T1	Object-based method	Built Up Terminal	1.49	54,912.48	45.00	11.98	N/A	N/A
		Built Up Infrastructure	18.21	667,458.85	36.51	7.18		
		Built Up Other Depots	6.49	238,144.91	-10.93	-16.19		
		Built Up Ancillary/Gen.	1.49	54,913.21	-197.24	33.22		
		Vegetation/Barren land	42.44	1,555,024.00	-14.37	-1.63		
		Forest	29.84	1,093,451.81	42.90	1.45		
LC08_L2SP_136045_20131030_20200912_02_T1	Object-based method	Built Up Terminal	0.68	25,176.04	-78.44	-10.62	N/A	N/A
		Built Up Infrastructure	22.21	814,011,88	19.85	10.35		
		Built Up Other Depots	6.51	238,571.81	0.30	-12.06		
		Built Up Ancillary/Gen.	23.35	855,576.46	275.18	93.71		
		Vegetation/Barren land	14.48	530,794.28	-107.53	-28.11		
		Forest	32.74	1,199,789.06	9.61	3.40		
LC08_L2SP_136044_20141220_20200910_02_T1	Object-based method	Built Up Terminal	0.53	19,443.17	-24.92	-13.48	N/A	N/A
		Built Up Infrastructure	44.00	1,611,302.25	68.36	21.95		
		Built Up Other Depots	3.30	121,222.90	-67.94	-23.24		
		Built Up Ancillary/Gen.	2.66	97,772.71	-217.22	31.52		
		Vegetation/Barren land	22.30	816,831.71	43.18	-13.85		
		Forest	27.19	996,156.46	-18.57	-1.00		
LC08_L2SP_136045_20151223_20200908_02_T1	Object-based method	Built Up Terminal	0.52	19,166.79	-1.90	-11.55	-1.90	N/A
		Built Up Infrastructure	37.04	1,357,335.65	-17.22	15.42	-17.21	
		Built Up Other Depots	5.00	183,399.25	41.55	-12.44	41.55	
		Built Up Ancillary/Gen.	6.21	227,607.31	84.78	40.39	84.78	
		Vegetation/Barren land	22.72	832,368.05	1.86	-11.23	1.86	
		Forest	28.49	1,043,815,83	4.67	-0.01	4.67	
LC08_L2SP_136045_20161225_20200905_02_T1	Object-based method	Built Up Terminal	1.65	60,602.78	115.47	6.59	56.78	N/A
		Built Up Infrastructure	27.48	1,007,018.44	-29.85	8.95	-23.53	
		Built Up Other Depots	6.23	228,368.17	-7.67	-7.52	31.77	
		Built Up Ancillary/Gen.	15.92	583,189.80	94.14	48.07	89.46	
		Vegetation/Barren land	23.29	853,482.08	2.47	-9.27	2.17	
		Forest	25.40	930,574.33	-11.48	-1.68	-3.40	
						$\%_{c_1}$	$\%_{c_2}$	$\%_{c_3}$

$$(\%_a) = \ln\frac{y_n}{y_0};\ (\%_b) = \rightarrow \text{CAGR}(t_0, t_n) = \left(\frac{V(t_n)}{V(t_0)}\right)^{\frac{1}{t_n - t_0}} - 1;\ (\%_{c_{1,2,3}}) = 1/\text{T}\ \ln\frac{y_{n\cdots\bar{k}+T}}{y_{n\cdots\bar{k}}} \rightarrow \%_{c_1} = 2009 \cdots y_{\bar{k}}\ ;\ \%_{c_2} = 2014 \cdots y_{\bar{k}};\ \%_{c_3} = 2017 \cdots y_{\bar{k}}$$

Table 9.2 Classification areal percentage employing OLI Landsat 8 datasets in accordance with an object-based method.

Data	Classification method	Cover types	Index (%a)	Area (mq)	Change year (%b)	Annual change rate (%c)		
LC08_L1TP_136044_20171126_20200902_02_T1	Object-based method	Built Up Terminal	1.03	37,958.48	-47.12	-0.12	22.14	N/A
		Built Up Infrastructure	30.55	1,119,372.75	10.59	9.16	-12.16	
		Built Up Other Depots	5.77	211,378.88	-7.67	38.77	18.62	
		Built Up Ancillary/Gen.	12.23	448,294.47	-1.89	38.77	50.85	
		Vegetation/Barren land	25.45	932,376.15	8.86	-7,00	4.40	
		Forest	24.94	913,980.11	-1.82	-1.69	-2.87	
LC08_L2SP_136045_20181231_20200830_02_T1	Object-based method	Built Up Terminal	0.72	26,275.09	-35.80	-4.08	7.65	-35.80
		Built Up Infrastructure	28.35	1,040,949.26	-7.47	7.31	-10.98	-7.47
		Built Up Other Depots	6.56	239,652.88	12.83	-5.27	17.17	12.83
		Built Up Ancillary/Gen.	12.00	440,299.88	-1.89	34.25	37.66	-1.89
		Vegetation/Barren land	25.57	938,830.82	0.47	-6.17	3.42	0.47
		Forest	26.84	985,275.21	7.34	-0.69	-0.32	7.34
LC08_L2SP_136045_20191218_20201023_02_T1	Object-based method	Built Up Terminal	0.50	18,331.46	-36.46	-7.32	-1.16	-36.13
		Built Up Infrastructure	6.33	232,430.09	-150.00	-8.41	-38.77	-78.70
		Built Up Other Depots	8.00	293,492.64	19.84	-2.76	17.71	16.33
		Built Up Ancillary/Gen.	33.45	1,227,848.96	102.51	41.07	50.63	50.30
		Vegetation/Barren land	15.52	569,851.54	-54.15	-10.55	-7.24	-24.72
		Forest	36.21	1,329,223.06	29.94	2.36	5.72	18.64
LC08_L2SP_136044_20201204_20210313_02_T1	Object-based method	Built Up Terminal	0.74	27,260.78	39.20	-3.09	5.56	-11.02
		Built Up Infrastructure	11.04	405,301.00	55.62	-2.59	-23.04	-33.92
		Built Up Other Depots	8.24	302,763.46	2.95	-2.24	15.25	11.87
		Built Up Ancillary/Gen.	29.98	1,100,732.87	-10.95	36.34	40.37	29.88
		Vegetation/Barren land	9.03	331,502.95	-54.15	-14.51	-15.06	-34.53
		Forest	40.96	1,503,810.80	12.32	3.27	6.82	16.53
LC09_L2SP_136045_20211215_20220120_02_T1	Object-based method	Built Up Terminal	1.17	42,846.43	45.81	0.98	11.31	3.18
		Built Up Infrastructure	20.83	763,103.03	63.48	2.91	-10.68	-9.57
		Built Up Other Depots	6.65	243,818.30	-21.43	-3.84	10.00	3.54
		Built Up Ancillary/Gen.	18.57	680,315.35	-47.89	29.32	27.76	10.44
		Vegetation/Barren land	22.08	808,852.16	89.41	-5.85	-0.14	-3.55
		Forest	30.69	1,124,502.70	-28.86	0.59	1.72	5.18
LC08_L1TP_136044_20220516_20220519_02_T1	Object-based method	Built Up Terminal	1.11	40,506.80	-5.26	0.50	9.24	1.49
		Built Up Infrastructure	0.28	904,837.29	-430.93	-30.45	-63.21	-93.84
		Built Up Other Depots	7.69	272,250.00	14.53	-2,43	10.57	5.74
		Built Up Ancillary/Gen.	12.39	452,313.41	-40.46	23.95	19.23	0.25
		Vegetation/Barren land	23.25	848,564.13	5.16	-5,00	0.52	-1.80
		Forest	30.99	1,131,044.94	0.97	0.62	1.63	4.34
LC09_L2SP_136045_20220727_20220729_02_T1	Object-based method	Built Up Terminal	1.17	43,062.76	5.26	0.84	8.79	2.12
		Built Up Infrastructure	23.62	865,347.61	443.50	3.39	-6.91	-4.28
		Built Up Other Depots	7.86	288,156.53	2.18	-2.10	9.64	5.15
		Built Up Ancillary/Gen.	8.47	310,201.93	-38.03	19.53	12.86	-6.12
		Vegetation/Barren land	30.90	1,131,810.651	28,44	-2.61	3.62	3.23
		Forest	27.96	1,024,285.58	-10.28	-0.15	0.31	1.9
						$\%_{c_1}$	$\%_{c_2}$	$\%_{c_3}$

$(\%_a) = \ln \frac{y_n}{y_0}$; $(\%_b) = \rightarrow \mathrm{CAGR}(t_0, t_n) = \left(\frac{V(t_n)}{V(t_0)}\right)^{\frac{1}{t_n - t_0}} - 1$; $(\%_{c_{1,2,3}}) = 1/T \ln \frac{y_{n\cdots\bar{k}+T}}{y_{n\cdots\bar{k}}} \rightarrow \%_{c_1} = = 2009 \cdots y_{\bar{k}}$; $\%_{c_2} = 2014 \cdots y_{\bar{k}}$; $\%_{c_3} = 2017 \cdots y_{\bar{k}}$

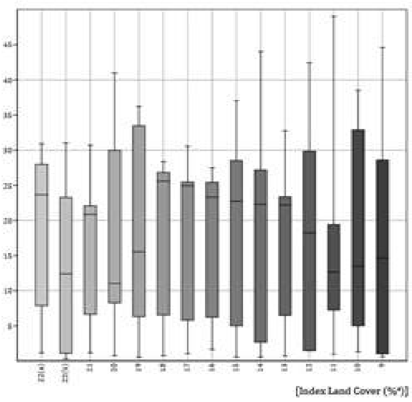

Figure 57. Surface quantitative distribution, quartile method based, with $q_{1/4} = 0.28$ %, 2022(b), $q_{1/3} = 49.00$

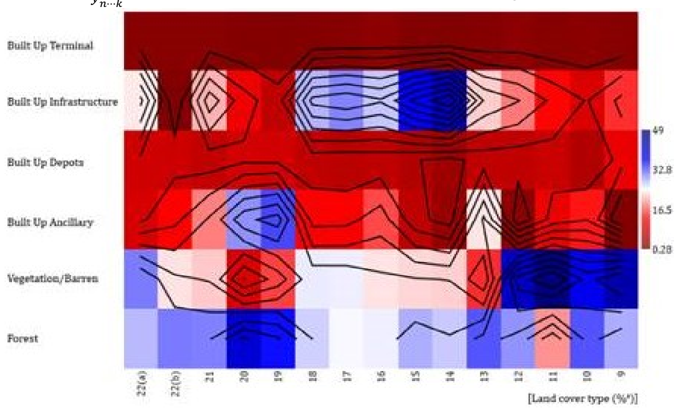

Figure 58. Pearson correlation of sensed cover types. Highest appreciation visualizes a considerable BM Terminal growth, between 2014-18 with a 115.47 %b increase during the

%, 2011. Lowest Median IQR = 10.04 %, 2020, highest IQR = 18.785, 2018.

2016; the prosperous vegetation reported in 2011 a 14.37 %b decrease, despite of the previous years. In the biennial 17-18, BU Depots increased by volume.

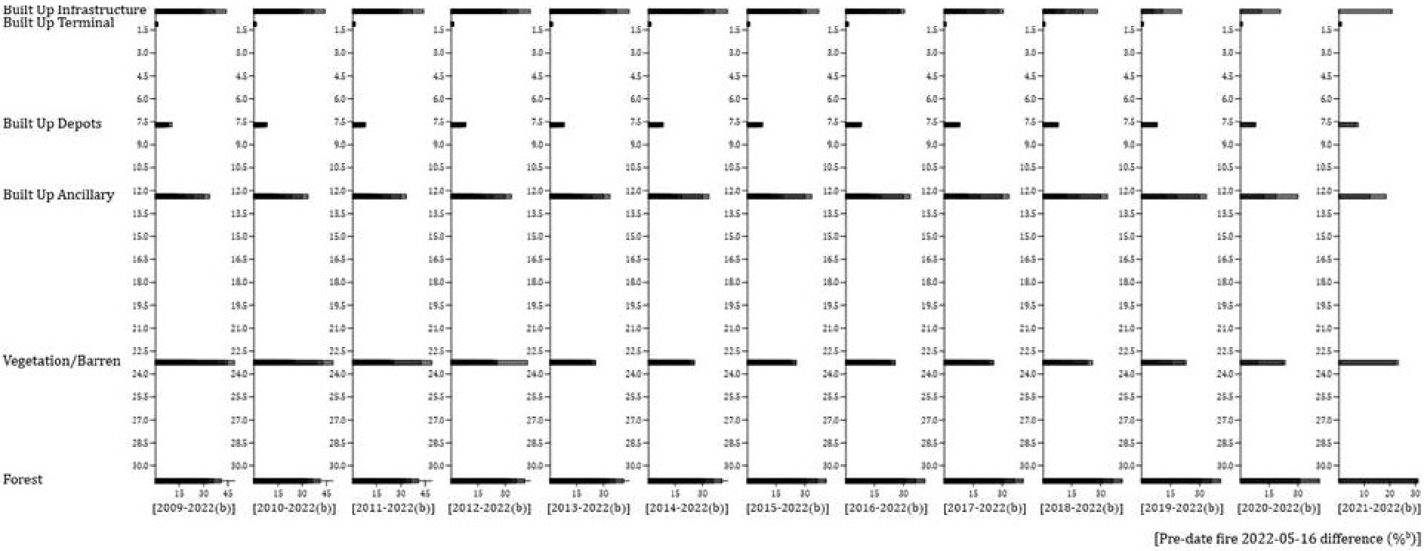

Figure 59. Area-based variation over the years. 2022(b) chosen as discriminator.

2.6. MLE ISODATA Cluster

The performance of the latest stage of this research regards an unsupervised classification on a biennial series of 2022 (a) and (b) input raster bands. The MLE has spatially analyzed a final, nearly total, area completed by many internal sprawls. The remaining LULC classes have been visually also interpretated by exclusion of this automatic identification. The Whole Iso cluster-based analysis did not present any error or image patches during the processing nor the achieved result with a set of initial training data that matched positively in accordance with such dual outcome. All pixels are classified to the nearest class until the number of pixels in each class changes by less than pixel variation is reached.

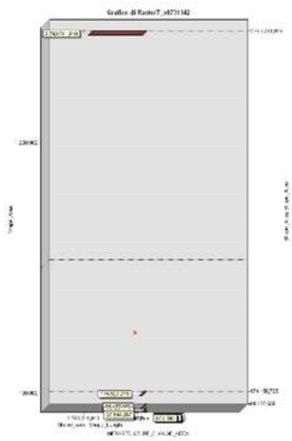

Figure 60. The list of input raster bands reported, over a total area, 2,835,058.22 m², 285 shapes; the lowest is equal to 222.13 m², the highest to 2,793,741.92 m². The residual extension is visually scattered and quantitatively listed as follows below.

RasterT_x0731142, 01/10/2022, Pagina 1

OBJECTID *	Shape *	Id	gridcode	Shape_Length	Shape_Area
1	Poligono	1	1	89.424364	444,262053
2	Poligono	2	1	119.232486	888,524105
3	Poligono	3	1	59.616243	222,131026
4	Poligono	4	1	59.616243	222,131026
5	Poligono	5	1	59.616243	222,131026
6	Poligono	6	0	59.616243	222,131026
7	Poligono	7	1	238.464972	1777,04821
8	Poligono	8	1	89.424364	444,262053
9	Poligono	9	1	268.273093	2109,534365
10	Poligono	10	1	59.616243	222,131026
11	Poligono	11	1	178.848729	1332,786158
12	Poligono	12	1	208.65685	1777,048211
13	Poligono	13	1	59.616243	222,131026
14	Poligono	14	1	59.616243	222,131026
15	Poligono	15	1	59.616243	222,131026
16	Poligono	16	1	59.616243	222,131026
17	Poligono	17	1	59.616243	222,131026
18	Poligono	18	1	59.616243	222,131026
19	Poligono	19	1	59.616243	222,131026
20	Poligono	20	0	59.616243	222,131026
21	Poligono	21	1	89.424364	444,262053
22	Poligono	22	1	178.848729	1554,917184
23	Poligono	23	1	119.232486	888,524105
24	Poligono	24	1	387.505579	3554,096421
25	Poligono	25	1	59.616243	222,131026
26	Poligono	26	1	59.616243	222,131026
27	Poligono	27	1	149.040607	888,524105
28	Poligono	28	1	89.424364	444,262053
29	Poligono	29	1	387.505579	3554,09642
30	Poligono	30	1	89.424364	444,262053
31	Poligono	31	1	59.616243	222,131026
32	Poligono	32	1	59.616243	222,131026
33	Poligono	33	1	298.081215	2665,572316
34	Poligono	34	0	59.616243	222,131026
35	Poligono	35	1	59.616243	222,131026
36	Poligono	36	1	59.616243	222,131026
37	Poligono	37	1	178.848729	1332,786158
38	Poligono	38	1	59.616243	222,131026
39	Poligono	39	0	119.232486	888,524105
40	Poligono	40	0	59.616243	222,131026
41	Poligono	41	0	59.616243	222,131026
42	Poligono	42	1	864.435822	9329,503105
43	Poligono	43	1	119.232486	888,524105
44	Poligono	44	1	89.424364	444,262053
45	Poligono	45	0	59.616243	222,131026
46	Poligono	46	1	119.232486	888,524105
47	Poligono	47	1	59.616243	222,131026
48	Poligono	48	1	208.65685	1777,04821
49	Poligono	49	1	59.616243	222,131026
50	Poligono	50	1	59.616243	222,131026
51	Poligono	51	1	89.424364	444,262053
52	Poligono	52	0	59.616243	222,131026
53	Poligono	53	0	59.616243	222,131026
54	Poligono	54	1	89.424364	444,262053
55	Poligono	55	1	1669.254802	20435,233457
56	Poligono	56	1	59.616243	222,131026
57	Poligono	57	1	59.616243	222,131026
58	Poligono	58	0	89.424364	444,262053
59	Poligono	59	1	59.616243	222,131026
60	Poligono	60	0	59.616243	222,131026
61	Poligono	61	0	59.616243	222,131026
62	Poligono	62	1	59.616243	222,131026
63	Poligono	63	1	268.273093	2143,41129
64	Poligono	64	1	1311.557344	20658,185417
65	Poligono	65	1	2145.185715	21137,658071
66	Poligono	66	1	178.848729	1332,786158
67	Poligono	67	1	89.424364	444,262053
68	Poligono	68	1	59.616243	222,131026
69	Poligono	69	1	2384.649696	56421,280682
70	Poligono	70	1	89.424364	444,262053
71	Poligono	71	0	59.616243	222,131026
72	Poligono	72	1	89.424364	444,262053
73	Poligono	73	0	59.616243	222,131026
74	Poligono	74	0	59.616243	222,131026
75	Poligono	75	1	327.889336	3331,965395

RasterT_x0731142, 01/10/2022, Pagina 2

OBJECTID *	Shape *	Id	gridcode	Shape_Length	Shape_Area
76	Poligono	76	1	59,616243	222,131026
77	Poligono	77	1	149.040607	888,524105
78	Poligono	78	1	119.232486	666,393079
79	Poligono	79	1	119.232486	888,524105
80	Poligono	80	1	59,616243	222,131026
81	Poligono	81	0	119.232486	666,393079
82	Poligono	82	1	119.232486	666,393079
83	Poligono	83	1	89,424364	444,262053
84	Poligono	84	1	59,616243	222,131026
85	Poligono	85	1	59,616243	222,131026
86	Poligono	86	1	59,616243	222,131026
87	Poligono	87	1	119.232486	666,393079
88	Poligono	88	1	417.3137	3887,703547
89	Poligono	89	1	59,616243	222,131026
90	Poligono	90	1	59,616243	222,131026
91	Poligono	91	1	89,424364	444,262053
92	Poligono	92	0	208.65685	1554,917184
93	Poligono	93	0	59,616243	222,131026
94	Poligono	94	1	59,616243	222,131026
95	Poligono	95	1	89,424364	444,262053
96	Poligono	96	1	59,616243	222,131026
97	Poligono	97	1	59,616243	222,131026
98	Poligono	98	1	59,616243	222,131026
99	Poligono	99	0	59,616243	222,131026
100	Poligono	100	1	178.848729	1110,655132
101	Poligono	101	1	89,424364	444,262053
102	Poligono	102	1	89,424364	444,262053
103	Poligono	103	1	89,424364	444,262053
104	Poligono	104	1	59,616243	222,131026
105	Poligono	105	1	89,424364	444,262053
106	Poligono	106	0	149.040607	1332,786158
107	Poligono	107	1	59,616243	222,131026
108	Poligono	108	0	59,616243	222,131026
109	Poligono	109	1	178.848729	1110,655132
110	Poligono	110	0	89,424364	444,262053
111	Poligono	111	1	59,616243	222,131026
112	Poligono	112	0	119.232486	666,393079
113	Poligono	113	0	59,616243	222,131026
114	Poligono	114	1	149.040607	888,524105
115	Poligono	115	1	59,616243	222,131026
116	Poligono	116	0	119.232486	666,393079
117	Poligono	117	0	59,616243	222,131026
118	Poligono	118	0	178.848729	1110,655132
119	Poligono	119	0	59,616243	222,131026
120	Poligono	120	0	89,424364	444,262053
121	Poligono	121	1	89,424364	444,262053
122	Poligono	122	0	89,424364	444,262053
123	Poligono	123	1	178.848729	1332,786158
124	Poligono	124	1	59,616243	222,131026
125	Poligono	125	1	59,616243	222,131026
126	Poligono	126	1	89,424364	444,262053
127	Poligono	127	1	149.040607	888,524105
128	Poligono	128	1	149.040607	888,524105
129	Poligono	129	1	59,616243	222,131026
130	Poligono	130	0	178.848729	1332,786158
131	Poligono	131	1	59,616243	222,131026
132	Poligono	132	0	89,424364	444,262053
133	Poligono	133	0	59,616243	222,131026
134	Poligono	134	1	208.65685	1777,04821
135	Poligono	135	1	59,616243	222,131026
136	Poligono	136	0	327.889336	3331,965395
137	Poligono	137	1	59,616243	222,131026
138	Poligono	138	0	178.848729	1110,655131
139	Poligono	139	1	2076,95296	35540,064309
140	Poligono	140	1	178.848729	1777,048211
141	Poligono	141	0	178.848729	1332,786158
142	Poligono	142	1	89,424364	444,262053
143	Poligono	143	1	89,424364	444,262053
144	Poligono	144	1	119.232486	666,393079
145	Poligono	145	1	59,616243	222,131026
146	Poligono	146	1	89,424364	444,262053
147	Poligono	147	1	59,616243	222,131026
148	Poligono	148	1	59,616243	222,131026
149	Poligono	149	1	59,616243	222,131026
150	Poligono	150	1	89,424364	444,262053

RasterT_x0731142, 01/10/2022, Pagina 3

OBJECTID *	Shape *	Id	gridcode	Shape_Length	Shape_Area
151	Poligono	151	0	59,616243	222,131026
152	Poligono	152	0	89,424364	444,262053
153	Poligono	153	0	59,616243	222,131026
154	Poligono	154	1	89,424364	444,262053
155	Poligono	155	1	89,424364	444,262053
156	Poligono	156	0	149,040607	888,524105
157	Poligono	157	1	59,616243	222,131026
158	Poligono	158	0	59,616243	222,131026
159	Poligono	159	0	89,424364	444,262053
160	Poligono	160	1	327,889336	2887,703342
161	Poligono	161	1	298,081215	3331,965394
162	Poligono	162	1	417,3137	5331,144631
163	Poligono	163	1	59,616243	222,131026
164	Poligono	164	1	268,273093	1999,179237
165	Poligono	165	1	59,616243	222,131026
166	Poligono	166	0	119,232486	666,393079
167	Poligono	167	1	59,616243	222,131026
168	Poligono	168	0	59,616243	222,131026
169	Poligono	169	1	59,616243	222,131026
170	Poligono	170	1	59,616243	222,131026
171	Poligono	171	1	59,616243	222,131026
172	Poligono	172	1	59,616243	222,131026
173	Poligono	173	1	89,424364	444,262053
174	Poligono	174	0	59,616243	222,131026
175	Poligono	175	1	89,424364	444,262053
176	Poligono	176	1	208,65685	1554,917184
177	Poligono	177	1	894,243644	10218,02721
178	Poligono	178	1	119,232486	888,524105
179	Poligono	179	1	89,424364	444,262053
180	Poligono	180	1	59,616243	222,131026
181	Poligono	181	0	178,848729	1110,655132
182	Poligono	182	1	59,616243	222,131026
183	Poligono	183	1	89,424364	444,262053
184	Poligono	184	1	59,616243	222,131026
185	Poligono	185	1	59,616243	222,131026
186	Poligono	186	1	149,040607	1110,655132
187	Poligono	187	0	59,616243	222,131026
188	Poligono	188	1	59,616243	222,131026
189	Poligono	189	0	59,616243	222,131026
190	Poligono	190	1	119,232486	888,524105
191	Poligono	191	1	59,616243	222,131026
192	Poligono	192	1	1699,062923	19325,399289
193	Poligono	193	1	89,424364	444,262053
194	Poligono	194	0	238,464972	2443,441289
195	Poligono	195	1	59,616243	222,131026
196	Poligono	196	1	178,848729	1110,655132
197	Poligono	197	1	149,040607	1332,786158
198	Poligono	198	1	178,848729	1110,655132
199	Poligono	199	1	119,232486	888,524105
200	Poligono	200	1	59,616243	222,131026
201	Poligono	201	0	119,232486	666,393079
202	Poligono	202	1	59,616243	222,131026
203	Poligono	203	0	59,616243	222,131026
204	Poligono	204	1	59,616243	222,131026
205	Poligono	205	1	59,616243	222,131026
206	Poligono	206	1	59,616243	222,131026
207	Poligono	207	1	59,616243	222,131026
208	Poligono	208	1	298,081215	2443,441289
209	Poligono	209	1	298,081215	3554,096421
210	Poligono	210	1	119,232486	666,393079
211	Poligono	211	1	238,464972	1999,179237
212	Poligono	212	1	89,424364	444,262053
213	Poligono	213	1	59,616243	222,131026
214	Poligono	214	0	59,616243	222,131026
215	Poligono	215	1	59,616243	222,131026
216	Poligono	216	1	89,424364	444,262053
217	Poligono	217	0	89,424364	444,262053
218	Poligono	218	1	119,232486	666,393079
219	Poligono	219	1	476,929943	4664,751553
220	Poligono	220	1	59,616243	222,131026
221	Poligono	221	1	59,616243	222,131026
222	Poligono	222	0	59,616243	222,131026
223	Poligono	223	1	59,616243	222,131026
224	Poligono	224	0	178,848729	1110,655132
225	Poligono	225	1	59,616243	222,131026

RasterT_x0731142, 01/10/2022, Pagina 4

OBJECTID *	Shape *	Id	gridcode	Shape_Length	Shape_Area
226	Poligono	226	1	59.616243	222,131026
227	Poligono	227	1	536.546188	4442,620526
228	Poligono	228	1	119.232486	666,393079
229	Poligono	229	1	178.848729	1777,04821
230	Poligono	230	0	149.040607	888,524105
231	Poligono	231	1	119.232486	666,393079
232	Poligono	232	1	208.65685	2221,310263
233	Poligono	233	0	59.616243	222,131026
234	Poligono	234	1	178.848729	1110,655132
235	Poligono	235	1	178.848729	1332,786158
236	Poligono	236	1	864.435822	12438,337473
237	Poligono	237	0	59.616243	222,131026
238	Poligono	238	1	1758.679188	27544,247262
239	Poligono	239	1	536.546188	5331,144631
240	Poligono	240	1	119.232486	666,393079
241	Poligono	241	1	59.616243	222,131026
242	Poligono	242	1	238.464972	2443,441289
243	Poligono	243	1	89.424364	444,262053
244	Poligono	244	1	59.616243	222,131026
245	Poligono	245	1	59.616243	222,131026
246	Poligono	246	1	89.424364	444,262053
247	Poligono	247	1	59.616243	222,131026
248	Poligono	248	1	59.616243	222,131026
249	Poligono	249	1	119.232486	888,524105
250	Poligono	250	1	59.616243	222,131026
251	Poligono	251	1	59.616243	222,131026
252	Poligono	252	0	59.616243	222,131026
253	Poligono	253	1	59.616243	222,131026
254	Poligono	254	1	89.424364	444,262053
255	Poligono	255	1	59.616243	222,131026
256	Poligono	256	1	119.232486	888,524105
257	Poligono	257	1	59.616243	222,131026
258	Poligono	258	1	119.232486	888,524105
259	Poligono	259	1	89.424364	444,262053
260	Poligono	260	1	178.848729	1554,917184
261	Poligono	261	1	119.232486	888,524105
262	Poligono	262	1	89.424364	444,262053
263	Poligono	263	1	357.697458	3998,358473
264	Poligono	264	1	59.616243	222,131026
265	Poligono	265	1	178.848729	1777,04821
266	Poligono	266	1	625.970551	7774,586921
267	Poligono	267	0	59.616243	222,131026
268	Poligono	268	1	119.232486	888,524105
269	Poligono	269	0	149.040607	1332,786158
270	Poligono	270	1	178.848729	1554,917184
271	Poligono	271	0	59.616243	222,131026
272	Poligono	272	1	59.616243	222,131026
273	Poligono	273	0	268.273093	2221,310263
274	Poligono	274	1	119.232486	888,524105
275	Poligono	275	1	59.616243	222,131026
276	Poligono	276	0	59.616243	222,131026
277	Poligono	277	0	149.040607	1110,655131
278	Poligono	278	0	59.616243	222,131026
279	Poligono	279	0	149.040607	1332,786158
280	Poligono	280	0	119.232486	666,393079
281	Poligono	281	1	5031.583804	174156,734623
282	Poligono	282	1	89.424364	444,262053
283	Poligono	283	0	149.040607	888,524105
284	Poligono	284	1	10462.853834	175927,772835
285	Poligono	285	0	59.616243	222,131026
286	Poligono	286	1	119.232486	666,393079
287	**Poligono**	**287**	**0**	**54806,555737**	**2793741,917944**

Table 10. Cluster-based reporting of the infrastructural change.

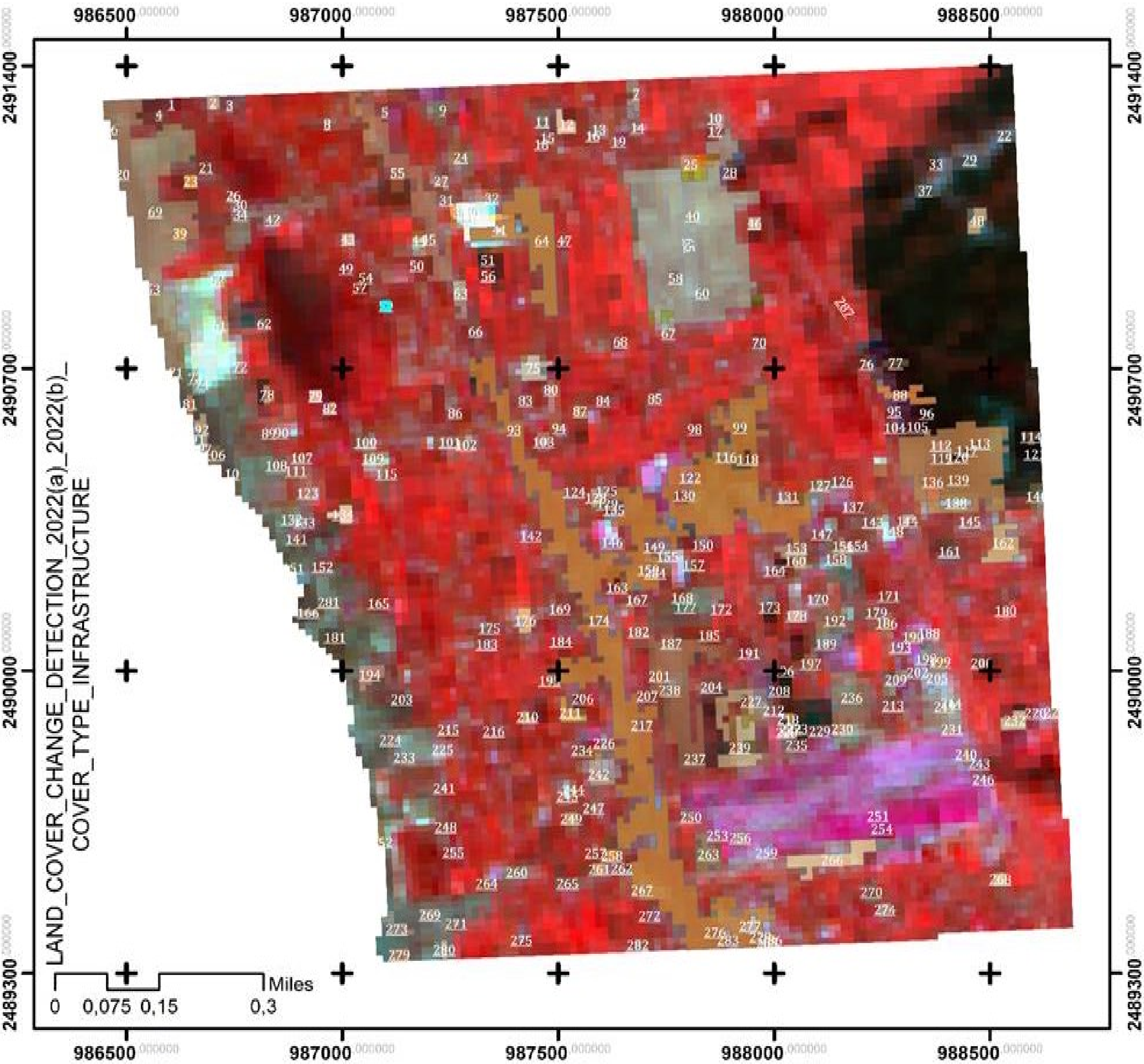

Figure 61. Target shapefile iso cluster performed. Reference image is the near-infrared (NIR) 3-4-5 2022(b) raster composite, with the near IR band, interpreted as addressed to the unseen matter, that clearly displays zones interested by chlorophyll and its vital health.

3. Conclusions

The persistence and continuity between past, present and future of this coastal fabric of Bangladesh is an example of many other dynamics that occurred along the coasts of the Mediterranean basin. The permanence of those tangible and intangible traces of the heritage consists of a key testimony regarding the safeguarding of urban identity, as this continuous renewal has stratified and superimposed in the form of stratigraphy. The expressed versatility of the installation of industrial landmarks, together with the slum's phenomena, in their dissemination of urban sprawl, the agricultural-forestry fabric, has recently attracted in Bangladesh, international stakeholders linked to the recovery of ships. This coastal activity was reasoned in a cooperation curated and named "The theme of the Mediterranean" (Casamonti M., 2006) was the subject of activities led by the Order of Architects of Naples, with the hope of ratifying a "Charter of Mediterranean cities on architectural quality ("*Carta delle città del Mediterraneo sulla qualità architettonica*"), and discussed the historic shipbuilding of Naples, and its related starting point towards the horizon of this sea and the Atlantic ocean. On the thematic section illustrated by the "Annals of Architecture and

Cities Foundation" ("*Fondazione Annali dell'Architettura e delle Città*"), the shipbuilding activity was made tangible and has characterized the bond of this Mediterranean capital over the past centuries. The exhibition mentioned in this volume, entitled "The large ships in the port of Naples" was set up on the first floor in the Royal Palace of Naples, and with a wide digression on the coastal landmarks, entitled "Mediterranean Nomadism", unfolded in the same courtyard which took place in 2007. In this exhibition, the connotation of an itinerant and evolving naval coastal landscape was precisely placed, which characterized not only Naples but the entire Italian peninsula; examples of this exhibition have been made known through the images of the "*Cantieri Riuniti di Monfalcone*", the "*Cantiere di Castellamare*", the "*Cantieri Siciliani di Palermo*". The applicability of this analysis on this coastal passage, so rapidly becoming a humanitarian problem of today's industrialized Bangladesh, therefore wants to contribute to the awareness and defence against land consumption, promoting on a sub-regional level, to their annual census, to promote the elevation of those landscape classes, such as rurality, the colour plane, and intangible heritage to contribute to the competent orders, such as the Superintendence and Cultural Heritage. Furthermore, the promotion of our professional order at this event highlighted a role, in the dimension of interior architecture, which was sadly neglected, and that is of the progressivism inaugurated by Italian architects in the Mediterranean, for those buildings more possibly similar to ships, without that European rational obstinacy, but of authentic poetics between man and the infinite spatial dimension of the sea: "Mediterraneanism", labelled between 1928 and 1932, and declared by Le Corbusier on the back of the book "*Poesie per Algeri*" in which Algiers, Paris, Barcelona and Rome, were the lighthouses of the Mediterranean. Regarding coastal defence in Italy, the Higher Institute for Environmental Protection and Research, (Department of Protection of Inland and Marine Waters, 2022), constantly works with reference to the publication on the effects caused to the coasts, of those potential solid transports and, in general, to soil erosion. The numerical model, with forecast up to 48 hours, "*Sistema Idro Meteo Mare*" (SIMM), is offered free of charge on this Italian institutional portal, with crucial navigation data, i.e. a Finite Element Model (FEM), aiming at the most congenial forecast for the sea level values in the Venice lagoon.

Acknowledgements

The scope of this quantitative research is aimed to enlighten the modern approach of the image-and remote-sensing applications in favor of sustainable planning of port areas, regarding LULC and Infrastructure change. This crisis object-based urban detection, together with the extensive yearly accuracy and statistical models, intended for fine-tuned evaluations - specifically: "*Valutazione Impatto Ambientale*" (VIA) (Environmental Impact Assessment, EIA) and "*Valutazione Impatto Strategica*" (VAS) (Strategic Environmental Assessment, SEA) - is addressed to the contribution, as novel research, in favor of the Port Authority strategic planning. The authors contributed to this work in different ways: Salvatore Polverino conducted the primary research and wrote the first draft and Antonio Coppola assisted with data orientation and policy-making boundary spanners, also providing critical feedback on the manuscript. The authors also give proper credit as enlisted in the references section. Besides, this research benefitted from a research fund regulated within the Department Training and Internationalization c/o *Ordine degli Architetti, Pianificatori, Paesaggisti, Conservatori di Napoli e Provincia Napoli, Italy,* whose international commitment was inaugurated by ex-President Arch. Raffaele Sirica (1995-1997) in occasion of the Habitat II program by the second United Nations Conference on Human Settlements, taken place from 3-14 June 1996, in Instanbul, Turkey. The authors express appreciation to the esteemed specialists who have shown their support for the archival initiative and governmental consultation: in-Office President, Prof. Dr. Arch. Lorenzo Capobianco, former President, Prof. Arch. Paolo Pisciotta and President of the Disciplinary Board, Arch. Gennaro Polichetti, and Prof. Dr. Arch. Leonardo Di Mauro, former and honorary President.

Data availability statement

The original contributions presented in the study are included in the article/supplementary material, further inquiries can be directed to the corresponding authors. Sitakunda images (pp. 20-21-22) are a result from Google street maps and/or other Imagery.

Ethics statements

Studies involving animal subjects: No animal studies are presented in this manuscript. Studies involving human subjects: No human studies are presented in this manuscript. Inclusion of identifiable human data: no potentially identifiable human images or data is presented in this study.

Conflict of Interests

The authors declare no conflict of interest. The numerical conclusions, as well as their numerical processing, have not accountability in the role, design, collection, or interpretation of data but aims at demonstrating adequate and modern methodologies that are derive from three branches in the process of Training and Internationalization at the *Ordine degli Architetti Pianificatori Paesaggisti Conservatori di Napoli e Provincia*: architecture of landscape, engineering for the territory and agronomy. The Department does not promote any misconduct, e.g., 95/46/EC and Regulation (EC) No 45/2001 (EC) No 45/2001, by endorsing: the reintroduction of historical components ecologically suitable, a sustainable land use perspective and data extraction techniques without animal experimentation and environmental invasive footprint in accordance with the rigorous Italian legislation for the landscape. No research institution, e.g., university teaching, has ever been involved in the research.

References

Abdullah, Hasan Muhammad, M. Golam Mahboob, Mehmuna R. Banu, e Dursun Zafer Seker. (May 2013) «Monitoring the Drastic Growth of Ship Breaking Yards in Sitakunda: A Threat to the Coastal Environment of Bangladesh». *Environmental Monitoring and Assessment* 185, fasc. 5: 3839–51. https://doi.org/10.1007/s10661-012-2833-4.

Acharya, Tri Dev, In Tae Yang, e Dong Ha Lee. (August 2018). «Land Cover Classification of Imagery from Landsat Operational Land Imager Based on Optimum Index Factor». *Sensors and Materials* 30, fasc. 8: 1753. https://doi.org/10.18494/SAM.2018.1866.

Aickin, M. (1990). Maximum likelihood estimation of agreement in the constant predictive probability model, and its relation to Cohen’s kappa. *Biometrics*. Vol. 46, pp. 293–302

Alam, Shawkat, e Abdullah Faruque. (July 2014). «Legal Regulation of the Shipbreaking Industry in Bangladesh: The International Regulatory Framework and Domestic Implementation Challenges». *Marine Policy* 47: 46–56. https://doi.org/10.1016/j.marpol.2014.01.022.

Amen, M. A. (2021). The Assessment of Cities Physical Complexity through Urban Energy Consumption. Civil Engineering and Architecture, 9(7), 2517–2527. https://doi.org/10.13189/cea.2021.090735

Aziz Amen, M. (2022). The effects of buildings’ physical characteristics on urban network centrality. Ain Shams Engineering Journal, 13(6), 101765. https://doi.org/10.1016/j.asej.2022.101765

Amen, M. A., & Nia, H. A. (2020). The Effect of Centrality Values in Urban Gentrification Development: A Case Study of Erbil City. Civil Engineering and Architecture, 8(5), 916–928. https://doi.org/10.13189/cea.2020.080519

Amen, M. A., Afara, A., & Nia, H. A. (2023). Exploring the Link between Street Layout Centrality and Walkability for Sustainable Tourism in Historical Urban Areas. Urban Science, 7(2), 67. https://doi.org/10.3390/urbansci7020067

Bangladesh University of Engineering and Technology. (October 2012). Air Pollution Reduction Strategy for Bangladesh Final Report, Department of Environment Government of Bangladesh.

Barua, Uttama, Erik Wiersma, Maruf Billah, e Mehedi Ansary. (2018). «Fire Evacuation Safety in Bangladesh RMG Factories: A Comparison of Standards and Non-Compliance Issues of Means of Escape», *Symposium on Safety in Garment Industry, Five Years After Rana Plaza At: Dhaka.*

Byrt, Ted, Janet Bishop, e John B. Carlin. (1993). «Bias, Prevalence and Kappa». *Journal of Clinical Epidemiology* 46, n. 5: 423–29. https://doi.org/10.1016/0895-4356(93)90018-V.

Brennan, R. and D. Prediger. (1981). Coefficient kappa: Some uses, misuses, and alternatives. *Educational and Psychological Measurement*. Vol. 41, pp. 687–699.

Casamonti, Marco. (*2006). Overview sull’architettura italiana: Sud : learning from south : paesaggi urbani del Mediterraneo*. 1. ed. Milano: Motta architettura.

Bangladesh Forest Department. (December 2016). Climate Resilient Participatory Afforestation and Reforestation Project, Bangladesh Forest Department. Technical Study for Mapping of Potential Greenbelt Zone in the Coastal Regions of Bangladesh, Final Report. Center for Environmental and Geographic Information Services. Bangladesh.

Cai, Guoyin, Huiqun Ren, Liuzhong Yang, Ning Zhang, Mingyi Du, e Changshan Wu. (Luglio 2019). «Detailed Urban Land Use Land Cover Classification at the Metropolitan Scale Using a Three-Layer Classification Scheme». *Sensors* 19, fasc. 14): 3120. https://doi.org/10.3390/s19143120.

Cohen, Jacob. (April 1960) «A Coefficient of Agreement for Nominal Scales». *Educational and Psychological Measurement* 20, n. 1: 37–46. https://doi.org/10.1177/001316446002000104.

Cohen, Jacob. (1968). «Weighted Kappa: Nominal Scale Agreement Provision for Scaled Disagreement or Partial Credit.» *Psychological Bulletin* 70, n. 4: 213–20. https://doi.org/10.1037/h0026256.

Congalton, R.G., Oderwald, R.G., Mead, R.A., (1983). Assessing Landsat classification accuracy using discrete multivariate analysis statistical techniques. *Photogramm. Eng. Remote. Sens*. 49 (12), 1671–1678.

Congalton, Russell G. (2001). «Accuracy Assessment and Validation of Remotely Sensed and Other Spatial Information». *International Journal of Wildland Fire* 10, n. 4: 321. https://doi.org/10.1071/WF01031.

Department of Sociology, Mangalore University, Mangalagangotri-574199, Karnataka, India, Md. Shohel Mahmud, Vinay Rajath D., Department of Business Administration, Noakhali Science and Technology University, Noakhali-3814, Bangladesh., Mst. Nusrat Jahan, e Department of Food and Nutrition, National College of Home Economics

(University of Dhaka), Dhaka-1207, Bangladesh. (July 2018)«Health Issues of Female Garment Workers: Evidence from Bangladesh». *Journal of Population and Social Studies* 26, fasc. 3: 181–94. https://doi.org/10.25133/JPSSv26n3.013.

Dipartimento Tutela delle Acque Interne e Marine. (2022). Capitolo 3, “Il CLIMA ONDOSO A LARGO DELLE COSTE ITALIANE”. Servizio Difesa delle Coste. APAT Agenzia per la Protezione dell’Ambiente e per I servizi Tecnici.

Feizizadeh, Bakhtiar, Sadrolah Darabi, Thomas Blaschke, e Tobia Lakes. (June 2022)«QADI as a New Method and Alternative to Kappa for Accuracy Assessment of Remote Sensing-Based Image Classification». *Sensors* 22, fasc. 12: 4506. https://doi.org/10.3390/s22124506.

Fleiss, J., J. Cohen, and B. Everitt. (1969). Large sample standard errors of kappa and weighted kappa. *Psychological Bulletin*. Vol. 72, No. 5, pp. 323–327.

Foody, G. (June 2010)«Assessing the Accuracy of Remotely Sensed Data: Principles and Practices: Book Reviews». *The Photogrammetric Record* 25, n. 130: 204–5. https://doi.org/10.1111/j.1477-9730.2010.00574_2.x.

Foody, Giles M. (2020). «Explaining the Unsuitability of the Kappa Coefficient in the Assessment and Comparison of the Accuracy of Thematic Maps Obtained by Image Classification». *Remote Sensing of Environment* 239: 111630. https://doi.org/10.1016/j.rse.2019.111630.

Hudson, W.D. and Ramm, C.W. (1987) Correct Formulation of the Kappa Coefficient of Agreement, *Photogrammetric Engineering and Remote Sensing*, 53, 421-422.

Humayun Kabir K. (2012) «An Investigation into Geospatial Tools for a Multipurpose Cadastre: A Digital Cadastre Prototype for Bangladesh». *LAP LAMBERT Academic Publishing.* ISBN 978-3845472904

Hussain, Sajjad, Muhammad Mubeen, e Shankar Karuppannan. (June 2022)«Land Use and Land Cover (LULC) Change Analysis Using TM, ETM+ and OLI Landsat Images in District of Okara, Punjab, Pakistan». *Physics and Chemistry of the Earth, Parts A/B/C* 126: 103117. https://doi.org/10.1016/j.pce.2022.103117.

Islam, Md. Nazrul, e André van Amstel. (2022). a c. di. *India II: Climate Change Impacts, Mitigation and Adaptation in Developing Countries*. Springer Climate. Cham: Springer International Publishing,. https://doi.org/10.1007/978-3-030-94395-0.

Islam, Md. Deen, Warren A. Kaplan, Veronika J. Wirtz, e Kevin P. Gallagher. (March 2022): «The Social Costs of Success: The Impact of World Trade Organization Rules on Insulin Prices in Bangladesh upon Graduation from Least Developed Country Status». *Asian Development Review* 39, fasc. 01: 239–79. https://doi.org/10.1142/S0116110522500093.

Kuveždić Divjak, Ana, Almin Đapo, e Boško Pribičević. (2020). «Cartographic Symbology for Crisis Mapping: A Comparative Study». *ISPRS International Journal of Geo-Information* 9, n. 3: 142. https://doi.org/10.3390/ijgi9030142.

Landis, J. Richard, e Gary G. Koch. (1977). «The Measurement of Observer Agreement for Categorical Data». *Biometrics* 33, n. 1: 159. https://doi.org/10.2307/2529310.

Matlhodi, Botlhe, Piet K. Kenabatho, Bhagabat P. Parida, e Joyce G. Maphanyane. (September 2019). «Evaluating Land Use and Land Cover Change in the Gaborone Dam Catchment, Botswana, from 1984–2015 Using GIS and Remote Sensing». *Sustainability* 11, fasc. 19: 5174. https://doi.org/10.3390/su11195174.

McNamara, Derek, e William Mell. (January 2022). «Towards the Use of Remote Sensing for Identification of Building Damage, Destruction, and Defensive Actions at Wildland-Urban Interface Fires». *Fire Technology* 58, n. 1: 641–72. https://doi.org/10.1007/s10694-021-01170-6.

Mohamed, Abdelbaseer A., Rūta Ubarevičienė, e Maarten van Ham. (September 2022). «Morphological Evaluation and Regeneration of Informal Settlements: An Experience-Based Urban Design Approach». *Cities* 128: 103798. https://doi.org/10.1016/j.cities.2022.103798.

Nippon Koei Co. & Chiyoda U-tech Co.. (January 2018). Data Collection Survey on Computerization of Gas and Power Network Infrastructure in Bangladesh. People’s Republic of Bangladesh Ministry of Power, Energy and Mineral Resources.

Olofsson, Pontus, Giles M. Foody, Stephen V. Stehman, e Curtis E. Woodcock. (2013). «Making Better Use of Accuracy Data in Land Change Studies: Estimating Accuracy and Area and Quantifying Uncertainty Using Stratified Estimation». *Remote Sensing of Environment* 129): 122–31. https://doi.org/10.1016/j.rse.2012.10.031.

People’s Republic of Bangladesh Ministry of Power, Energy and Mineral. (January 2018). Resources Data Collection Survey on Computerization of Gas and Power Network Infrastructure in Bangladesh, Final Report. *Japan International Cooperation Agency (JICA).*

Polverino, Salvatore. (2022). «Fire and Explosion Machine Learning Model for the Port of Los Angeles - California Safety Code and NFPA for Fire-Break Zoning». *Journal of Mediterranean Cities* 2, fasc. 1: 58–83. https://doi.org/10.38027/mediterranean-cities_vol2no1_5.

Pontius, Robert Gilmore, e Marco Millones. (August 2011)«Death to Kappa: Birth of Quantity Disagreement and Allocation Disagreement for Accuracy Assessment». *International Journal of Remote Sensing* 32, fasc. 15: 4407–29. https://doi.org/10.1080/01431161.2011.552923.

Rahman Kaunain. Reviewed by: Mullard Saul. (2021). Bangladesh: Overview of corruption and anticorruption Focus on ready-made garments (RMG), health, environment, and anticorruption actors.

Rahman, Md. Ashabur, Mansura Akter, e Wahidul Shemon. (January 2019). «A National and International Regulatory Framework for Establishing Sustainable Shipbreaking Industry in Bangladesh» 3: 87–108.

Razzaque, M., & Rahman, J. (2019). Bangladesh's Apparel Exports to the EU: Adapting to Competitiveness Challenges Following Graduation from Least Developed Country Status. Commonwealth Secretariat. https://www.researchgate.net/profile/JillurRahman/publication/333092701_Bangladesh%27s_Apparel_Exports_to_the_EU_Adapting_to_Competitiveness_Challenges_Following_Graduation_from_Least_Developed_Country_Status/links/5cdb239a299bf14d95986c52/Bangladeshs-Apparel-Exports- to-the-EU-Adapting-to-Competitiveness-Challenges-Following-Graduation-from- Least-Developed-Country-Status.pdf Accessed April 2023.

Rosenfield, G.H., Fitzpatrick-Lins, K., (1986). A coefficient of agreement as a measure of thematic classification accuracy. *Photogramm. Eng. Remote. Sens.* 52 (2), 223–227

Saini, Varinder, e Reet Kamal Tiwari. (September 2020). «A Systematic Review of Urban Sprawl Studies in India: A Geospatial Data Perspective». *Arabian Journal of Geosciences* 13, n. 17: 840. https://doi.org/10.1007/s12517-020-05843-4.

Saha, Pritam, Rajib Mitra, Kunal Chakraborty, e Maitreyee Roy. (April 2022). «Application of Multi Layer Perceptron Neural Network Markov Chain Model for LULC Change Detection in the Sub-Himalayan North Bengal». *Remote Sensing Applications: Society and Environment* 26: 100730. https://doi.org/10.1016/j.rsase.2022.100730.

Stehman, S.V., & Foody, G.M. (2019). Key issues in rigorous accuracy assessment of land cover products. *Remote Sensing of Environment*. https://doi.org/10.1016/j.rse.2019.05.018.

The Hazardous Wastes and Shipbreaking Waste Management Rules. (2011). Bangladesh Gazette. http://doe.portal.gov.bd/sites/default/files/files/doe.portal.gov.bd/page/5134b0c1_ee8b_4dd6_8bf8_5e829f18a4aa/Hazardous_waste_and_ship_breaking_waste_management_rules_2011.pdf.

Thron, Christopher, e Vincent Miller. (2015). «Persistent Confusions about Hypothesis Testing in the Social Sciences». *Social Sciences* 4, n. 2 361–72. https://doi.org/10.3390/socsci4020361.

Tran, Duy X., Filiberto Pla, Pedro Latorre-Carmona, Soe W. Myint, Mario Caetano, e Hoan V. Kieu. (February 2017)«Characterizing the Relationship between Land Use Land Cover Change and Land Surface Temperature». *ISPRS Journal of Photogrammetry and Remote Sensing* 124: 119–32. https://doi.org/10.1016/j.isprsjprs.2017.01.001.

Tuhin, Tanvir, N Chowdhury, M Karim, A Hoque, Mohammad Shariful Julfikar, e Bilton Basak. (2020). «ASSESSMENT OF THE ENVIRONMENTAL QUALITY OF SITAKUNDA SHIP BREAKING YARD».

Türk, Goksel. (1979). «Gt Index: A Measure of the Success of Prediction». *Remote Sensing of Environment* 8, n. 1: 65–75. https://doi.org/10.1016/0034-4257(79)90024-5.

Uddin Kamal Abu M. & Kaudstaal R. (December 2003). Delineation of the Coastal Zone. Program Development Office for Integrated Coastal Zone Management Plan (PDO-ICZMP).

Wadud, Zia, Fuad Yasin Huda, e Nizam Ahmed. (September 2014). «Assessment of Fire Risk in the Readymade Garment Industry in Dhaka, Bangladesh». *Fire Technology* 50 https://doi.org/10.1007/s10694-013-0349-2.

Wang, Ruci, Yuji Murayama, e Takehiro Morimoto. (April 2021)«Scenario Simulation Studies of Urban Development Using Remote Sensing and GIS: Review». *Remote Sensing Applications: Society and Environment* 22: 100474. https://doi.org/10.1016/j.rsase.2021.100474.